VOLUME 78 SEPARATE No. 122

PROCEEDINGS

AMERICAN SOCIETY
OF
CIVIL ENGINEERS

MARCH, 1952

AMERICAN SOCIETY OF CIVIL ENGINEERS FOUNDED 1852

ENGINEERING ASPECTS OF DIFFRACTION AND REFRACTION

By J. W. Johnson, M. ASCE

HYDRAULICS DIVISION

Headquarters of the Society
33 W. 39th St.
New York 18, N.Y.

PRICE $0.50 PER COPY

GUIDEPOST FOR TECHNICAL READERS

"Proceedings-Separates" of value or significance to readers in various fields are here listed, for convenience, in terms of the Society's Technical Divisions. Where there seems to be an overlapping of interest between Divisions, the same Separate number may appear under more than one item.

Technical Division	*Proceedings-Separate Number*
Air Transport	42, 43, 48, 52, 60, 93, 94, 95, 100, 103, 104, 108, 121 (Discussion: D-XXVIII, D-7, D-16, D-18, D-23, D-43)
City Planning	58, 60, 62, 64, 93, 94 99, 101, 104, 105, 115 (Discussion: D-16, D-23, D-43, D-60, D-62, D-65)
Construction	43, 50, 55, 71, 92, 94, 103, 108, 109, 113, 117, 121 (Discussion: D-3, D-8, D-17, D-23, D-36, D-40, D-71)
Engineering Economics	46, 47, 62, 64, 65, 68, 69, 95, 100, 104, 119 (Discussion: D-2, D-19, D-27, D-30, D-36, D-57)
Engineering Mechanics	41, 49, 51, 54, 56, 59, 61, 88, 89, 96, 116, 122 (Discussion: D-5, D-XXIII, D-XXV, D-18, D-24, D-33, D-34 D-49, D-54, D-61)
Highway	43, 44, 48, 58, 70, 100, 105, 108, 113, 120, 121 (Discussion: D-XXVIII, D-7, D-13, D-16, D-23, D-60)
Hydraulics	50, 55, 56, 57, 70, 71, 78, 79, 80, 83, 86, 92, 96, 106, 107, 110, 111, 112, 113, 116, 120 (Discussion: D-XXVII, D-9, D-11, D-19, D-28, D-29, D-56, D-70, D-71)
Irrigation	46, 47, 48, 55, 56, 57, 67, 70, 71, 87, 88, 90, 91, 96, 97, 98, 99, 102, 106, 109, 110, 111, 112, 114, 117, 118, 120 (Discussion: D-XXIII, D-3, D-7, D-11, D-17, D-19, D-25-K, D-29, D-30, D-38, D-40, D-44, D-47, D-57, D 70, D-71)
Power	48, 55, 56, 69, 71, 88, 96, 103, 106, 109, 110, 117, 118, 120 (Discussion: D-XXIII, D-2, D-3, D-7, D-11, D-17, D-19, D-25-K, D-30, D-38, D-40, D-44, D-70, D-71)
Sanitary Engineering	55, 56, 87, 91, 96, 106, 111, 118 (Discussion: D-10, D-29, D-37, D-56, D-60, D-70)
Soil Mechanics and Foundations	43, 44, 48, 94, 102, 103, 106, 108, 109, 115 (Discussion: D-4, D-XXVIII, D-7, D-43, D-44, D-56)
Structural	42, 49, 51, 53, 54, 59, 61, 66, 89, 100, 103, 109, 113, 116, 117, 119, 121, 122 (Discussion: D-3, D-5, D-8, D-13, D-16, D-17, D-21, D-23, D-24, D-25-K, D-32, D-33, D-34, D-37, D-39, D-42, D-49, D-51, D-54, D-59, D-61)
Surveying and Mapping	50, 52, 55, 60, 63, 65, 68, 121 (Discussion: D-60, D-65)
Waterways	41, 44, 45, 50, 56, 57, 70, 71, 96, 107, 112, 113, 115, 120 (Discussion: D-8, D-9, D-19, D-27, D-28, D-56, D-70, D-71)

A constant effort is made to supply technical material to Society members, over the entire range of possible interest. Insofar as your specialty may be covered inadequately in the foregoing list, this fact is a gage of the need for your help toward improvement. Those who are planning papers for submission to "Proceedings-Separates" will expedite Division and Committee action measurably by first studying the ASCE "Guide for Development of Proceedings-Separates" as to style, content, and format. For a copy of this Manual, address the Manager, Technical Publications, ASCE, 33 W. 39th Street, New York 18, N. Y.

The Society is not responsible for any statement made or opinion expressed in its publications

Published at Prince and Lemon Streets, Lancaster, Pa., by the American Society of Civil Engineers. Editorial and General Offices at 33 West Thirty-ninth Street, New York 18, N. Y. Reprints from this publication may be made on condition that the full title of paper, name of author, page reference, and date of publication by the Society are given.

Proceedings—Vol. 78 March, 1952 Separate No. 122

AMERICAN SOCIETY OF CIVIL ENGINEERS

Founded November 5, 1852

PAPERS

ENGINEERING ASPECTS OF DIFFRACTION AND REFRACTION

By J. W. Johnson,[1] M. ASCE

Synopsis

The design, construction, and operation of many coastal engineering works is considerably dependent on the principles of wave refraction and diffraction. This paper develops and illustrates principles that enable the estimation of wave conditions at specified points in shallow water or at the shore line. The wave characteristics can be developed from weather observations or forecasts, or from wave recorders.

The phenomenon of wave refraction on a shoaling bottom, together with its companion effects such as littoral currents, is discussed. Refraction of waves by currents is also considered, and formulas are developed that make possible the measurement of this effect under various conditions. Wave diffraction by breakwaters is an important consideration in the engineering design of harbor facilities. Means of measuring and locating the area in which the phenomenon will occur are given for conditions of semi-infinite breakwaters and also for breakwater gaps.

An appendix presents a summary of the basic theory of wave diffraction and illustrates the computations necessary for the construction of a diffraction diagram.

Introduction

The extensive research on the problems of waves, surf, and related phenomena that has been completed since the start of World War II, has yielded valuable design data for the practicing engineer. These extensions of the understanding of wave motion have, in many instances, replaced empirical methods dating back to the 1870's, in other instances, they have permitted the

Note.—Written comments are invited for publication; the last discussion should be submitted by **September 1, 1952.**

[1] Associate Prof. of Mech. Eng., Univ. of California, Berkeley, Calif.

analytical solution of problems that were still solved primarily by rather expensive hydraulic model studies. Results obtained from some of these analyses are frequently only qualitative in character, but even so, they provide a rational basis for planning shore protection and improvement. Additional research and its correlation with field observations are necessary; however, sufficient progress has been made so that the compilation of wave data for design purposes and wave refraction and diffraction analyses are approaching the status of a standard component of shore-line investigations. The application of these principles are of basic importance to the design engineer. In some instances these principles also have permitted the analytical reconstruction and explanation of unusual phenomena observed in the past.

Estimation of Wave Characteristics

In the design, construction, and operation of structures exposed to wave action, adequate information is necessary on the height and period of the waves that might be expected to occur in the locality under study. The waves most commonly considered are those generated by wind. The characteristics of such waves can be predicted with reasonable accuracy from known meteorological conditions. Other waves of importance in the design of structures in certain localities are harbor surges and tsunamies. The problem of surging[2] is not considered in this paper. Tsunami waves, like earthquakes, are as yet impossible to predict but are capable of causing considerable damage to shore-line structures in certain localities. Although brief reference to tsunami waves is made in this paper, wind-generated waves are considered of primary importance. Unless otherwise noted, this paper will be confined to a discussion of wind-generated waves.

Wave Characteristics from Weather Observations or Forecasts.—Workable relationships[3] between the characteristics of waves and a generating wind appear to be fairly well established. These relationships between the height and period of waves, the fetch, and the velocity and duration of the wind have been presented in convenient graphical form[4] and can be used with confidence in estimating wave heights. (Wave heights refer to the "significant" height; that is, the average of the highest one third of the waves.) Continuing observations, however, indicate that wave periods obtained by these graphs are generally lower than has been observed,[5, 6] and therefore, these graphs have been revised.[7]

The estimation of wave conditions may be made on the basis of either a forecast or a hindcast. If wind velocities and the fetch are estimated from a

[2] "Long-Period Waves in Harbors," by John H. Carr, *Proceedings-Separate No. 125*, ASCE, April, 1952.

[3] "Wind, Sea and Swell; Theory of the Relations for Forecasting," by H. U. Sverdrup and W. H. Munk, *Technical Report in Oceanography No. 1, H. O. Publication No. 601*, Hydrographic Office, U. S. Navy, Washington, D. C., 1947.

[4] "Oscillatory Waves, Diagrams and Tables of Relationships Commonly Used In Investigations of Surface Waves," by R. L. Wiegel, *Bulletin*, Special Issue No. 1, Beach Erosion Board, Corps of Engrs., U. S. Army, Washington, D. C., July 1, 1948.

[5] "Comparison Between Recorded and Forecast Waves on the Pacific Coast," by J. D. Isaacs, and Thorndike Savelle, Jr., *Annals*, New York Academy of Science, Vol. 51, 1949, pp. 502–510.

[6] "Relationships Between Wind and Waves, Abbotts Lagoon, California," by J. W. Johnson, *Transactions*, Am. Geophysical Union, Vol. 31, 1950, p. 386.

[7] "Revised Forecasting Relationships," by C. L. Bretschneider, Second Conference on Coastal Eng., Houston, Tex., November, 1951.

weather chart, then an estimate of the wave conditions at a given locality at sea or at a coastal point also can be made. Such estimates usually are made where large-scale wind patterns are involved, such as in ocean areas. Wave forecasts are of particular importance to construction engineers when reliable information must be available on the wave and weather conditions that are likely to exist in a few hours. Such data are vital to the efficient planning of operations involving expensive construction equipment.

From the design engineer's point of view, a knowledge of the expected climate of a given location and a statistical summary of the height and period of waves from various directions is necessary. For localities along an open coast such summaries of wave conditions can be compiled by using the forecasting principles in a hindcasting procedure.[8] In this procedure the wave conditions for the winds and fetches, obtained from past weather charts, are estimated by use of the forecasting graphs previously mentioned and "roses" of wave heights and period are prepared.[9] In lakes and protected bays, it is usually unnecessary to resort to weather charts for past wind conditions, and local wind records of magnitude, duration, and direction are sufficient for estimating the wave conditions that might be expected to occur at any particular locality for various seasons of the year.[9]

The waves estimated from the foregoing procedures refer to deep-water conditions. For a shore point at which the waves must move through shallow water, considerable change in the wave characteristics might take place as a result of refraction and diffraction. Energy losses caused by bottom friction and flow in the permeable bed are of importance only in localities in which the waves must move for relatively long distances over a gently sloping bottom,[10, 11] such as on the Atlantic and the northwest Pacific coasts of the United States. In estimating wave conditions on lakes and bays, the variability of wave direction assumes considerable importance, since within the limits of the 30° angle of wave propagation a large range in fetch (and thus height and period) might be possible.[12] The variability of wave direction also is of importance since it materially affects the refraction of waves in passing an island or headland.

Wave Characteristics From Wave Recorders.—In addition to the forecasting method of compiling statistical data on wave conditions, recorders have been installed at numerous localities on the Atlantic, Gulf, and Pacific coasts.[13, 14, 15, 16]

---

[8] "Hindcasting Technique Provides Statistical Wave Data," by W. V. Burt and J. F. T. Saur, Jr., *Civil Engineering*, Vol. 18, 1948, pp. 47–49.

[9] "Action and Effect of Waves," by J. W. Johnson and J. D. Isaacs, *Western Construction News*, Vol. 23, 1948, pp. 97–102.

[10] "Loss of Wave Energy Due to Percolation in a Permeable Sea Bottom," by J. A. Putnam, *Transactions*, Am. Geophysical Union, Vol. 30, 1949, pp. 349–356.

[11] "Dissipation of Wave Energy by Bottom Friction," by J. A. Putnam and J. W. Johnson, *Transactions*, Am. Geophysical Union, Vol. 30, 1949, pp. 67–74.

[12] "Variability in Direction of Wave Travel," by R. S. Arthur, *Annals*, New York Academy of Sciences, Vol. 51, 1949, pp. 511–521.

[13] "Ocean Wave Measuring Instrument," by Joseph M. Caldwell, *Technical Memorandum No. 6*, Beach Erosion Board, Corps of Engrs., U. S. Army, Washington, D. C., October, 1948.

[14] "Measurement of Ocean Waves," by R. G. Folsom, *Transactions*, Am. Geophysical Union, Vol. 30, 1949, pp. 691–699.

[15] "Details of Shore-Based Wave Recorder and Ocean Wave Analyzer," by A. A. Klebba, *Annals*, New York Academy of Sciences, Vol. 51, May, 1949, pp. 533–544.

[16] "Wave Recorders," by Frank E. Snodgrass, *Proceedings*, First Conference on Coastal Eng., Council on Wave Research, Engineering Foundation, 1951.

The data from the recorders also provide a means of checking the forecasting technique previously discussed. The use of recorders in compiling statistical data on the frequency of wave occurrence of various heights and periods has the disadvantage that several years of records are necessary before average conditions may be determined. Even so, a year of record at a given station is of considerable value in giving important data for the design engineer.[17] Although the accuracy of the forecasting technique may be improved, recorders at certain key stations should always be maintained for checking purposes and for giving a record of the waves existing at any given instant. A forecaster benefits greatly, particularly, if a wave recorder is in operation in the forecasting office at the time the analysis is made. It is important to note that not all oceans are covered by weather maps; therefore, the hindcast procedure alone is insufficient. An example of this deficiency is evident along the coast of southern California, where, during a large percentage of time, waves reach the coast from generating areas to the south for which weather charts are not available. Wave recorders provide the only means of supplying complete data on wave conditions in this locality.

Wave Refraction on a Shoaling Bottom

General.—When waves move into shallow water, important transformations of all wave characteristics, except probably the wave period, take place. Waves approaching a shore line at an angle are bent, or refracted, because the inshore portion of the wave front travels at a lower velocity than does the portion in deeper water; consequently, the waves tend to swing around and conform to the bottom contours as shown in Fig. 1. The characteristics of the bottom topography, the wave period, and the wave direction in deep water determine the pattern of the wave crests in shallow water.[18, 19] The result of refraction is a change in the height and direction of the waves. With very irregular bottom conditions the heights may differ greatly between closely adjacent points along a coast.

The magnitude of the height and direction changes resulting from refraction can be estimated by use of a refraction diagram. Such a diagram may be considered to be a map showing the successive positions of a particular wave crest as it moves shoreward. If no energy flows laterally along the wave crest, then, in a steady state of wave motion, the same amount of energy should flow past all positions between any two sets of lines (orthogonals) that are everywhere perpendicular to the wave crests (Fig. 2). The power P transmitted by a train of sinusoidal waves is

$$P = C_g \times \frac{w}{8} \times b\,H^2 \qquad (1)$$

in which C_g = velocity of energy transmission; w = unit weight of water; b = length of crest; and H = wave height. Indicating the conditions in deep

[17] "Analysis of Data from Wave Recorders on the Pacific Coast of the United States," by R. L. Wiegel, *Transactions*, Am. Geophysical Union, Vol. 30, 1949, pp. 700–704.

[18] "Graphical Construction of Refraction Diagrams," by J. W. Johnson, M. P. O'Brien, and J. D. Isaacs, *H.O. Publication No. 605.*, Hydrographic Office, U. S. Navy, Washington, D. C., February, 1948.

[19] "Refraction of Ocean Waves: A Process Linking Underwater Topography to Beach Erosion," by W. H. Munk and M. A. Traylor, *Journal of Geology*, Vol. 55, 1947, pp. 1–26.

water by the subscript zero,

$$P = P_0 \qquad (2a)$$

or

$$H = H_0 \sqrt{\frac{C_{g0}}{C_g}} \sqrt{\frac{b_0}{b}} \qquad (2b)$$

The quantity $\sqrt{b_0/b}$ is termed the refraction coefficient and usually is designated as K_d. The quantity $\sqrt{C_{g0}/C_g}$ represents the effect of a change in depth

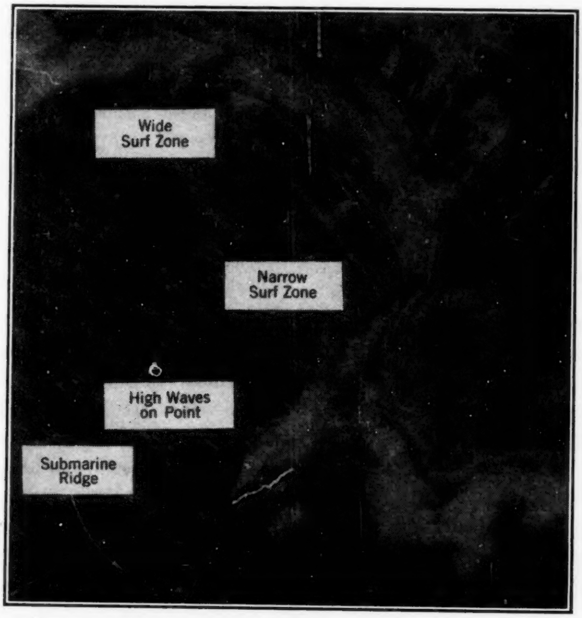

FIG. 1.—REFRACTION EFFECTS OF WAVES ON A SHOALING BOTTOM

on the wave height and is designated as D.[20] Then the wave height in any depth of water, may be written as:

$$H = H_0\, D\, K_d \qquad (3)$$

The values of the factors D and K_d depend on the depth and wave length and usually are opposite in effect. Refraction commonly tends to increase the length of the wave crest and to reduce the height, while the effect of D is to increase the height. With d representing the water depth, values of D for various values of relative depth (d/L_0) are available in published form.[4] In general, the D term is neglected in refraction studies. The values of K_d, on the other hand, can be determined from refraction diagrams for any given wave direction

[20] "Surface Water Wave Theories," by Martin A. Mason, *Proceedings-Separate No. 120*, ASCE, March, 1952.

and period. As illustrated by Fig. 3, the initial form of the wave is a straight line in the deep-water area. This figure shows that the graphical construction of a refraction diagram for a specified wave period consists simply of moving each point of the wave crest a distance perpendicular to the crest, equal to the wave velocity and multiplied by a convenient time interval.

The wave velocity for each depth is computed by the common wave equations:

$$L = C\,T \qquad (4)$$

and

$$C = \sqrt{\frac{g\,L}{2\,\pi}\tanh\frac{2\,\pi\,d}{L}} \qquad (5)$$

in which C = wave velocity; L = wave length; T = wave period; and d = depth. When the wave crests are completed, the initial wave crest in deep water is divided into equal increments, and lines are then drawn perpendicular to all intermediate crests from these division points to the shore as shown in Fig. 3. Refraction coefficients for any points in shallow water can be calculated by the equation $K_d = \sqrt{\frac{b_0}{b}}$ from orthogonal spacings measured on the diagram.

In addition to the wave-front method described briefly in the previous sections, refraction coefficients can be obtained by a method of drawing orthogonals directly. This latter method requires more experienced personnel than does the former; however, it has the advantage of greater speed of construction than the wave-front method, and a greater degree of accuracy is obtained in many instances. The details of both methods have been discussed elsewhere and, therefore, need not be considered in this paper.[18]

Refraction coefficients afford a convenient method of comparing wave heights at various localities. It is of interest to note that a convergence of orthogonals indicates a concentration of wave energy (large wave heights), whereas a divergence of orthogonals indicates a spreading out of energy, or low wave heights (Fig. 1). Thus, swell coming over a submarine valley usually experiences a decrease in height, and swell passing over a submarine ridge usually will be increased in height. Often the submarine topography is a continuation of the shore line and a submarine ridge frequently extends seaward at a point or headland. Similarly, a submarine valley often exists offshore of a bight or indentation in the coast line.

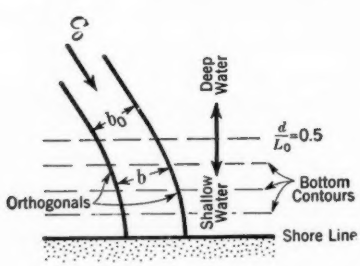

Fig. 2.—Wave Refraction Assuming Gradual Wave Velocity Change

Of great importance in the refraction of waves around headlands and islands is the variability of wave direction. Although waves are considered to be progressing in a certain direction, actually individual waves will be found

travelling in directions up to 30° either side of the average direction. This means that the penetration of waves to the lee of an island or headland may be much greater than that predicted from a refraction diagram based on the average direction of travel. A complete discussion of this phenomena has been presented by R. S. Arthur.[21]

Refraction diagrams are used primarily in connection with two types of investigation: (1) In the hindcasting and forecasting of wave or surf conditions; and (2) in the analysis and explanation of unusual wave conditions observed in the past. Depending on the use for which refraction diagrams are prepared, the coefficients usually are summarized in convenient tabular or graph form.

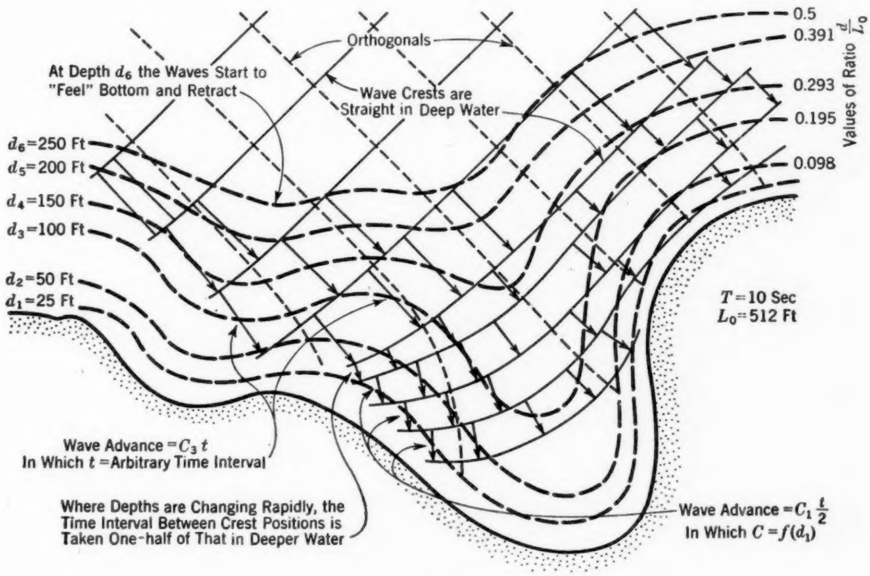

FIG. 3.—CONSTRUCTION OF A WAVE REFRACTION DIAGRAM

Some of the common uses of refraction diagrams and the presentation of pertinent data are presented in succeeding sections as well as elsewhere.[22]

Forecasting and Hindcasting of Wave Characteristics.—The technique of estimating wave conditions from synoptic weather charts has been discussed elsewhere.[20, 23] Such estimates pertain to deep-water conditions, but the transmission of these estimates into shallow water requires the use of refraction coefficients. The coefficients obtained from measurements made on refraction diagrams usually are summarized in graphical form. For example, when forecasts (or hindcasts) are being made for a single point on shore, a polar plot of

[21] "Variability in Direction of Wave Travel," by R. S. Arthur, *Annals*, New York Academy of Sciences, Vol. 51, Article 3, May, 1949, pp. 511–522.

[22] "Refraction and Diffraction Diagrams," by James W. Dunham, *Proceedings*, First Conference on Coastal Eng., Council on Wave Research, Engineering Foundation, 1951, pp. 33–49.

[23] "Wind Waves and Swell, Principles of Forecasting," by H. U. Sverdrup and W. H. Munk, *H. O. Publication 11,275*, Hydrographic Office, U. S. Navy, Washington, D. C., 1944.

K_d as a function of wave direction and period affords a rapid and convenient method of estimating wave heights at shore for any deep-water conditions, as indicated by Fig. 4. If forecasts are being made for several points along a coast, a convenient means of summarizing the data is a graph that shows K_d values plotted against distance along the shore for various wave periods. As shown in the typical example in Fig. 5, a separate curve for each wave direction is necessary. The basic data for plotting such summary diagrams, as illustrated by Fig. 4 and Fig. 5, are obtained most expeditiously by the method of plotting orthogonals directly, instead of by use of the wave-front method. It should be recognized that for those localities in which the tidal range is large, it may be necessary to construct separate refraction diagrams for different

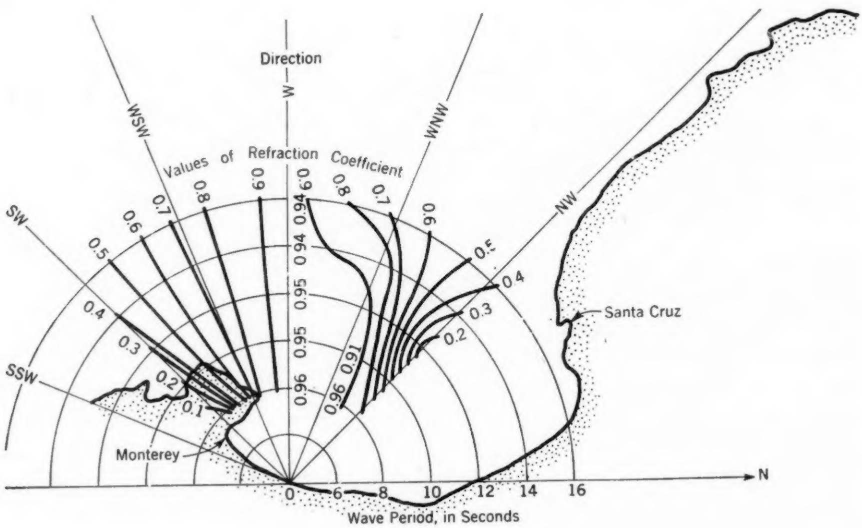

Fig. 4.—Refraction Diagram for Fort Ord, Calif.

stages of the tide. For most localities on the coast of the United States the tidal stage is approximately 5 ft, and refraction diagrams prepared for an average stage of tide usually will suffice for most investigations.

It is important to note that the assumption of constant wave energy between orthogonals is not valid after a wave breaks. If waves pass over a submerged reef, it may be necessary to examine this area critically to determine whether the wave breaks at some, or all, stages of the tide. Should breaking occur, wave heights beyond the reef would be lower than that determined by the use of K_d factors from a refraction diagram. As a wave passes over a reef, whether breaking occurs or not, the crest may divide into several crests, as shown in Fig. 6. Thus, the further refraction of the wave may be complex.

Littoral Currents.—When waves approach a shore line at an angle and then break upon the beach, a certain longshore component of the breaker velocity exists. Consequently, a littoral or longshore current is established in the direction of this component. It is this littoral current, combined with the

agitating action of the breaking waves, that is the primary factor in causing a movement of sand along a coast line. For a long straight beach the strength of the littoral current has been found by laboratory studies, supplemented by field observations,[24] to be

$$V = \frac{e}{2}\left[\sqrt{1 + \frac{3.45\, H^{\frac{1}{2}}_b}{e}\sin\alpha_b} - 1\right] \ldots\ldots\ldots\ldots\ldots (6)$$

in which $e = \dfrac{2.61\ m\ H_b \cos\alpha_b}{K\ T}$; V = littoral velocity in feet per second; m =

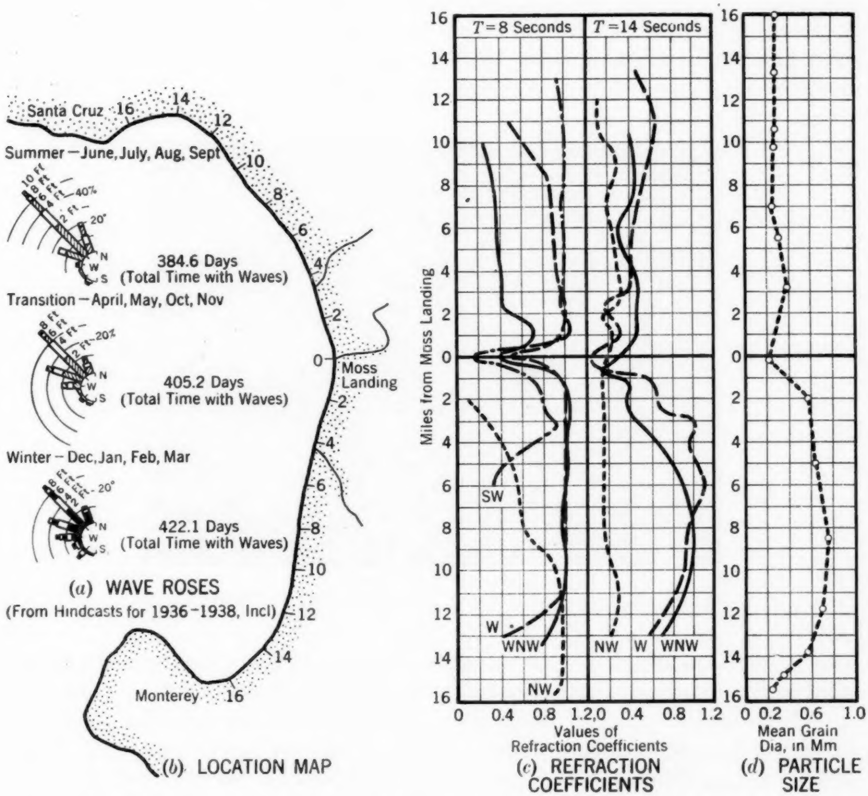

FIG. 5.—VARIATION OF REFRACTION COEFFICIENT AND SIZE OF BEACH MATERIAL ALONG SHORE LINE OF MONTEREY BAY

average beach slope; H_b = breaker height in feet; α_b breaker angle; T = wave period in seconds, and K = a dimensionless friction parameter depending on the hydraulic roughness of the bottom.[25, 26]

---

[24] "Prediction of Longshore Currents," by J. A. Putnam, W. H. Munk, and M. A. Traylor, *Transactions*, Am. Geophysical Union, Vol. 30, 1949, pp. 337–345.

[25] "Nearshore Circulation," by F. P. Shepard and D. L. Inman, *Proceedings*, First Conference on Coastal Eng., Council on Wave Research, Engineering Foundation, 1951, pp. 50–59.

[26] "Prediction and Variability of Longshore Currents," by D. L. Inman and W. H. Quinn, Second Conference on Coastal Eng., Houston, Tex., November, 1951.

For a given beach with a known slope, the strength of the littoral current can be estimated by first making a forecast (or hindcast) of deep-water wave conditions. The breaker height and angle can be determined from a refraction diagram constructed to show wave fronts up to the point of breaking. Knowing the period and deep-water height, the refraction diagram permits an estimate of the wave height at the breaker line as well as the measurement of the breaker angle. With these variables known the strength of the littoral current, therefore, can be calculated by using Eq. 6.

For a shore line that is subjected to waves of various periods from various directions, the littoral current may vary greatly in strength and direction throughout the year. If waves have more or less of a prevailing direction, the shore line, if composed of easily eroded material, will tend to adjust its alinement in such a manner that the shore line is parallel to the wave crests for the

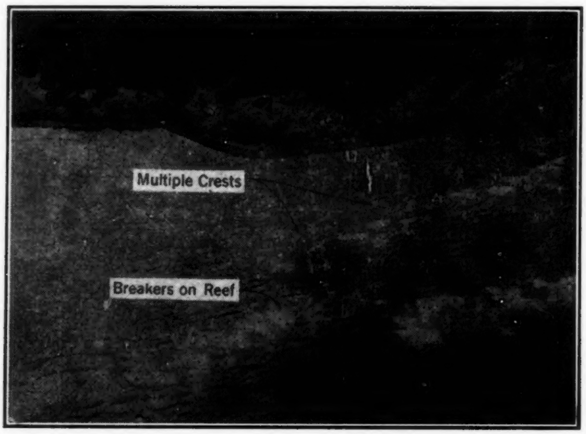

FIG. 6.—WAVE ACTION OVER AN ABRUPT CHANGE IN BOTTOM SLOPE

most severe conditions of wave attack—that is, the shore line tends to adjust itself to the condition of zero littoral current for the prevailing wave condition.

Monterey Bay, Calif., affords an excellent example of the relationship between bottom topography, shore-line alinement, and prevailing wave conditions. Thus, referring to Fig. 5, it is noted first that the wave rose, as prepared by the hindcasting technique,[3] shows a prevailing wave direction from the northwest. Refraction coefficients for waves of low period (8 sec) and high period (14 sec) from this direction were computed and plotted for various points along the shore line and are shown in Fig. 5. Also plotted in this diagram is the value of the mean grain diameter of the beach sand at various points along the shore line. The fact that the point of maximum values of K_d (mile 8–9 from Moss Landing) coincides with the point of maximum grain size is a significant factor and may be explained by recognizing that at those points along a shore line at which the refraction coefficient is high the littoral current is low, and vice versa. That is, the greater the refraction of the waves the

smaller is the refraction coefficient but the greater is the breaker angle and hence the larger the littoral current. The existence of a region of little or no littoral current, therefore, is a point of despoition and also a point of relatively large wave attack. Applying this reasoning to the southern half of Monterey Bay, it appears that at the section of the coast between miles 8 and 9 below Moss Landing, at which point the wave attack is the greatest, the littoral current is relatively weak. This reach is, therefore, a point of sand deposition from which the prevailing on shore winds remove material and build sand dunes along the back beach. The relatively large extent of wave attack is responsible for causing considerable sorting of the beach material by moving the finer sediment fractions into deep water and leaving the larger sizes on the shore. The relationship between sand size and degree of wave attack is well illustrated by Fig. 5.

To recognize that sand may move generally to certain localities on a shore line is of importance to construction engineers seeking a source of sand supply. As long as the removal of sand from such a source does not exceed the rate of supply by littoral drift, the shore line will remain stable with no serious erosion to adjacent beaches by such sand removal.

Analysis of Past Events.—On numerous occasions in the past, instances have occurred in which unusual wave conditions caused large amounts of damage to shore-line structures. At the time of occurrence of these conditions data were not available, in most instances, to explain completely the events that were observed to have occurred; however, with the increase in knowledge of wave action and related phenomena, many of these events have been explained to the satisfaction of those familiar with the problem. For example, from the knowledge of wave forecasting and wave refraction, Morrough P. O'Brien,[9, 27] M. ASCE has analyzed the occurrence in 1930 in which heavy wave action damaged a portion of the breakwater at Long Beach, Calif. At the time no wave action of unusual intensity was observed in adjacent areas. With the aid of refraction diagrams, it was shown that high-period waves generated many thousands of miles to the south (possibly in the southern hemisphere) must have approached the Long Beach area over a submarine ridge and concentrated directly on the breakwater. Because the submarine ridge was deeply submerged, it affected only waves of unusually long period, which thereby accounts for the fact that the phenomenon was a rare occurrence. In the case of wave damage at Long Beach, the serious beach erosion occurring at Santa Barbara, Calif., following the construction of the breakwater[27, 28] and other instances, refraction diagrams have played an important part in providing a rational basis for reasoning about the causes of damage and means of improvement.

Another example of the value of refraction diagrams in reconstructing and explaining past events is the tsunami wave of April 1, 1946, that caused considerable damage in the Hawaiian Islands and portions of the California coast. This wave resulted from an earthquake on the north face of the Aleutian trench, south of Unimak Island at latitude $53\frac{1}{2}°$ *N*, longitude between 163° and 164°.

---

[27] "Wave Refraction at Long Beach and Santa Barbara, California," by M. P. O'Brien, *Bulletin, No. 1*, Beach Erosion Board, Corps of Engrs., U. S. Army, Washington, D. C., January, 1950, p. 2.

[28] "Model Studies Made at the University of California River and Harbor Laboratory," by J. W. Johnson, *Transactions*, Am. Geophysical Union, Vol. 29, 1948, pp. 107–116.

The time of origin was 12:20.9 Greenwich civil time on April 1, 1946. The wave was observed at numerous points along the entire North and South American west coast, in the Hawaiian Islands, Tuamotu Archipelago, and at Bikini Atoll. Data on this wave, obtained from various sources, include information on arrival times from recording tide gages and the visual and photographic

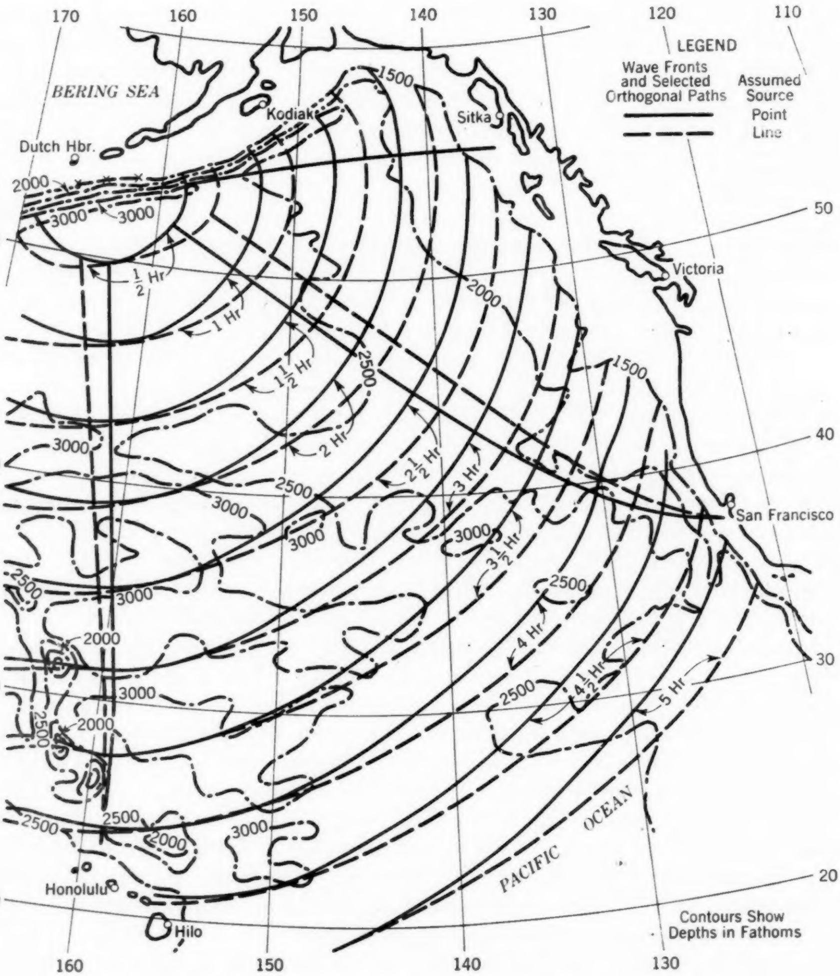

FIG. 7.—WAVE-FRONT DIAGRAM FOR SEISMIC SEA WAVE, APRIL 1, 1946

observations of wave heights and damage. The tide gage data, in particular, afford an opportunity for checking the shallow-water wave theory by comparing observed wave travel times to various points with those times calculated from a refraction diagram. In this instance, the basic theory for the construction of a refraction diagram is founded on the assumption that the waves are long

enough to conform to the shallow-water law for wave velocity ($C = \sqrt{g\,d}$). Thus, the velocity of propagation is independent of wave period. It is, therefore, evident that for a given seismic generating area, only one wave-front diagram is required to obtain the travel time to any point, and the results are applicable even in the absence of exact knowledge of the period or periods of the waves present in the generated train. The only point of uncertainty in the construction of a wave refraction diagram is the extent and shape of the initially generated wave front surrounding the disturbed area at the time of the earthquake. The location of the epicenter and the time of the first shock, however, are known with reasonable accuracy from seismographic data. Assuming both a point source and a line source at the epicenter, refraction diagrams were prepared by the wave-front method [29] and are shown in Fig. 7. The diagram for the line source was constructed on the arbitrary assumption that the source was approximately 168 nautical miles long and parallel to the face contours of the Aleutian Trench. The travel times for each position of the wave fronts are indicated in Fig. 7. A complete tabulation of travel times for those stations for which there was no circumstance casting any doubt on either the observed or computed results is given in Table 1. It is noted from this table that a maximum difference in travel time using the two types of epicenter was 19 min. This difference in travel time, when considered in the light of the total observed travel time (for example, the total observed time to San Francisco, Calif., was 5 hr 31 min) indicates a fair degree of accuracy.

TABLE 1.—DISCREPANCIES BETWEEN OBSERVED AND PREDICTED TRAVEL TIMES FOR SELECTED STATIONS

Station	Travel Time Differences in Min[a]	
	Point source	Line source
Honolulu, Hawaii	−7	−5
Sitka, Alaska	−21	−5
Clayoquot, British Columbia	−18	−2
Crescent City, Calif.	−19	−1
San Francisco, Calif.	−14	+4
Half Moon Bay, Calif.	+2	+20
Avila, Calif.	−7	+12
Port Hueneme, Calif.	−6	+11
La Jolla, Calif.	−14	−5

[a] Negative values indicate observed arrival in advance of theoretical indication.

Within practical limits it appears that the preceding analysis is valid as to travel time calculations and that the assumed line source gives results fitting the observations to within the order of accuracy of the analysis. It is of importance to recognize, however, that the waves as generated in a seismic disturbance constitute a wave group in which the first wave generated becomes progressively smaller with distance from the source and may even vanish, thus making the discrepancy between theoretical and observed arrival times even greater than that shown in Table 1. An examination of tide gage records[30] that recorded the tsunami of April 1, 1946, show that the wave of maximum

[29] "A Study Relating Data from the Seismic Sea Wave of April 1, 1946 to the Theory of its Propagation," by F. C. Roop, *Report HE-116-215*, Inst. of Eng. Research, Univ. of California, Berkeley, Calif., July 11, 1946 (unpublished).

[30] "Seismic Sea Wave of April 1, 1946, as Recorded on Tide Gages," by C. K. Green, *Transactions*, Am. Geophysical Union, Vol. 27, 1946, pp. 490–500.

height is, in general, the third or fourth wave in the group, and thus indicating that a group of waves did exist. The characteristic of a wave group is that the first wave eventually disappears and that the maximum wave height moves progressively back through the group.

Sufficient data are not available to make a comparison of measured and observed wave heights; however, it is perhaps reasonable to assume that, if the wave theory applies to estimates of travel time from refraction diagrams, then reasonably accurate estimates of relative wave heights at various points also could be made by determining refraction coefficients from these diagrams. In such estimates, however, the shoaling factor D in Eq. 3 undoubtedly should be considered.

Although the time and location of the source of tsunami waves are unpredictable, certain of the Pacific islands and parts of the Pacific coast of the United States have felt the damaging effects of such waves in the past, and there is no reason to expect that such effects will not be felt again in the future. A consideration of the basic principles of refraction permits an engineer to estimate the relative vulnerability of various localities along a given coast line to destruction by tsunami waves. Historically, it is known that certain cities have been greatly damaged several times by tsunami waves despite the fact that the waves originated in entirely different regions. Other near-by regions have never suffered damage. Hence, it appears that local underwater topography is particularly important in arriving at an evaluation of the safety of various localities against destructive action from tsunami sea waves coming from all possible directions. Such information is of importance in the orientation of breakwaters and other shore-line improvements, as well as in the structural design of the installations themselves. Actual damage at points at which the potential damage is great obviously will occur only if improvements of a character that waves can damage are in existence.

Refraction by Currents

When waves moving through still water encounter a current moving with, against, or at an angle to the wave direction, the waves undergo a change in length and steepness. In the case in which the waves meet a current at an angle, the waves also change their direction. In the forecasting of wave conditions there are two situations in which the refraction of waves by currents may be of practical importance. At tidal entrances, ebb currents run counter to the waves and increase the wave height and steepness, thereby adding to the hazards of navigation, while flood currents flatten out the waves. Large-scale ocean currents, such as the Gulf Stream, may have great effect on the height, length, and direction of the waves approaching the current discontinuity. In some instances, almost complete reflection of waves of certain periods will occur. In other instances, the waves have been forced by refraction to exceed their critical steepness and then to break.

The principal application of refraction methods is to predict the occurrence and height of breakers around a tidal entrance. The direction, height, and period of the waves in deep water are variable, the bottom contours usually are irregular, and the currents are variable throughout the tidal cycle. Under such

conditions quantitative forecasting by the purely analytical approach probably is not reliable, but a combination of theory and observation would be adequate for making forecasts of probable wave conditions at harbor entrances. In other instances the engineer might use the general principles of refraction by currents to design the shape of dredged tidal channels such that wave action within the channel will be reduced in magnitude.[31]

Surface waves in deep or shallow water are refracted by currents to an extent that depends on the initial wave velocity and direction and the strength of the current. Two common conditions are treated in the subsequent section which, for simplicity, is concerned only with deep-water waves.

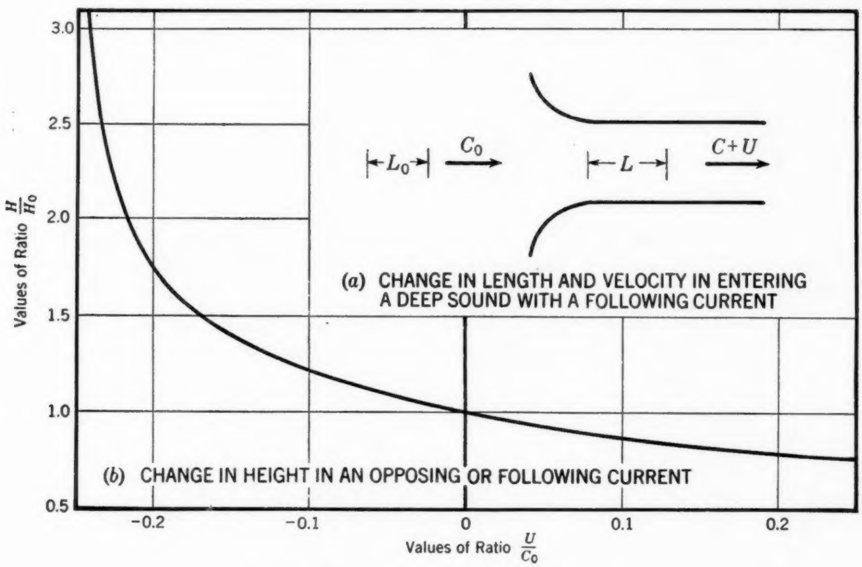

FIG. 8.—CHANGE IN WAVE CHARACTERISTICS

Waves Meeting or Following a Current:—When waves proceed from still, deep water into a deep sound in which a current runs directly with or against the advancing waves, the wave period remains constant, but the wave length, velocity, and height change.[32] Thus, referring to Fig. 8(*a*), if L_0 and C_0 represent the deep-water wave length and velocity, respectively, the wave length in the sound will be changed to a new value L. The wave velocity (relative to the water) corresponding to this wave length is $C^2 = \frac{(g\ L)}{(2\ \pi)}$; thus,

$$\frac{L}{L_0} = \left(\frac{C}{C_0}\right)^2 \qquad (7)$$

[31] "The Refraction of Surface Waves by Currents, A Discussion," by J. D. Isaacs, *Transactions*, Am. Geophysical Union, Vol. 29, 1948, pp. 739–742.

[32] "On Wave Heights in Straits and Sounds When Incoming Waves Meet a Strong Tidal Current," by H. U. Sverdrup, Scripps Inst. of Oceanography, La Jolla, Calif., April 20, 1944 (unpublished).

The wave velocity over the ground is equal to $(C + U)$, in which U is the velocity of the current in the sound. For constant period,

$$T = \frac{L_0}{C_0} = \frac{L}{(C + U)} \qquad (8)$$

From Eqs. 7 and 8,

$$\frac{C}{C_0} = \frac{1}{2}\left[1 \pm \sqrt{1 + 4\frac{U}{C_0}}\right] \qquad (9a)$$

Here the plus sign must be taken since C must equal C_0 where $U = 0$. Thus, if it is assumed that $\sqrt{1 + 4\frac{U}{C_0}} = a$,

$$\frac{C}{C_0} = \frac{1}{2}(1 + a) \qquad (9b)$$

and

$$\frac{L}{L_0} = \left(\frac{1 + a}{2}\right)^2 \qquad (10)$$

Considering Eqs. 7 and 9a it is seen that the effect of a following current is to increase the wave length, whereas the opposite effect results from an opposing current.

From a consideration of the advance of wave energy it can be shown that the ratio of the wave heights is

$$\frac{H}{H_0} = \sqrt{\frac{2}{a(1 + a)}} \qquad (11)$$

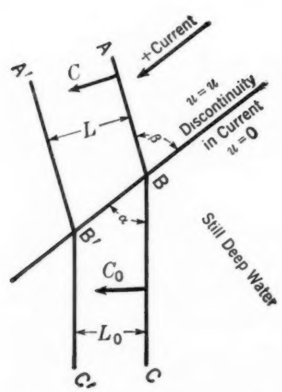

Fig. 9.—Relative Positions of Wave Crests Before and After Refraction by a Current

A plot of this equation showing the change in wave height in an opposing or following current is presented in Fig. 8(b). The effect on the wave steepness is obtained from a combination of Eqs. 10 and 11. Thus,

$$\frac{H}{L} = \frac{H_0}{L_0}\sqrt{\frac{2}{a(1 + a)}}\left[\frac{2}{(1 + a)}\right]^2 \qquad (12)$$

in which the wave steepness H/L in the sound is seen to depend on the initial steepness H_0/L_0 and on the ratio U/C_0. The waves in the sound will break when the value of H/L reaches the critical value of 1/7. As is apparent from Fig. 8(b), this condition takes place only when the waves meet an opposing current; that is, it is in this type of current that the height in the sound is increased over the deep-water height H_0.

Waves at an Angle to a Current.—Referring to Fig. 9, when a wave crest progresses from the position A B C in deep, still water across a current discontinuity to a position A′ B′ C′, changes in the wave length, height, and steepness

occur. This refraction by currents has two effects on the wave steepness. One effect is on the change in the wave length and the other is on the stretching or compressing of the wave crest. These effects may oppose or add, depending on whether the current direction is plus or minus. A treatment of the general

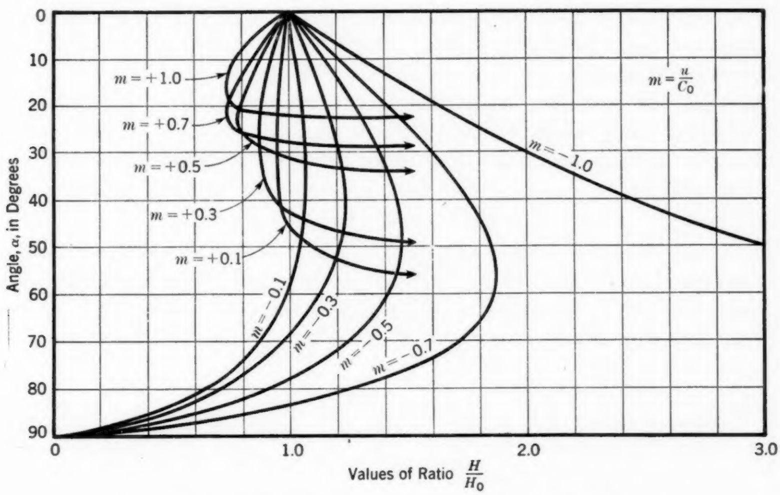

FIG. 10.—EFFECT OF REFRACTION BY CURRENTS ON WAVE HEIGHT

condition sketched in Fig. 9 shows[33] that the effect on wave length is

$$\frac{L}{L_0} = \frac{1}{\left(1 - \frac{U}{C_0 \sin \alpha}\right)^2} \qquad (13)$$

and the effect on wave steepness is

$$\frac{H}{L} = \frac{H_0}{L_0} \sqrt{\frac{\cos \alpha}{\cos \beta}\left[\frac{\left(1 - \frac{U}{C_0 \sin \alpha}\right)^6}{\left(1 + \frac{U}{C_0 \sin \alpha}\right)}\right]} \qquad (14)$$

or

$$\frac{H}{L} = \frac{H_0}{L_0} \quad (m) \qquad (15a)$$

This can be rewritten in the form,

$$\frac{H}{H_0} = \left(\frac{L}{L_0}\right) m \qquad (15b)$$

This combination of Eqs. 13 and 14 permits the preparation of a diagram (Fig. 10) that gives the change in wave height as a function of the strength and

[33] "The Refraction of Surface Waves by Currents," by J. W. Johnson, *Transactions*, Am. Geophysical Union, Vol. 28, 1947, pp. 867–874.

direction of the current compared to that of the incident wave. The most interesting feature of the curves presented in Fig. 10 is that, whether the waves enter an oncoming or a following current, they may increase in height (and, therefore, steepness) and then break. As an example, examination of Fig. 10 shows that when the value of $U/C_0 = +0.1$ (a following current) all waves of incident angle larger than about 58° will increase rapidly in height and, therefore, break. For higher plus values of U/C_0, the waves will break at much smaller incident angles.

The analyses given for waves meeting a current either directly or at an angle apply to deep-water conditions. A similar but more tedious analysis would result from an analysis of waves refracted by currents in shallow water.

Wave Diffraction

Wave diffraction is the phenomenon in which water waves are propagated into a sheltered region formed by a breakwater or similar barrier that interrupts a portion of a regular wave train. The principles of diffraction have considerable practical application in connection with the design of breakwaters. The phenomenon is analogous to the diffraction of light, sound, and electromagnetic waves, and theories for breakwater diffraction have been adapted from the theory of these phenomena. Two general types of diffraction problems usually are encountered: (*a*) The passage of waves around the end of a semi-infinite impermeable breakwater; and (*b*) the passage of waves through a gap in a breakwater. The complete theory for these two conditions appears to have been first developed during World War II.[34] These theories later were reworked and verified experimentally by model studies.[34, 35, 36] It appears, however, that the theory for the case of a semi-infinite breakwater was developed independently in France as early as 1942 and checked by field observations.[37] It also appears that simultaneously with these other studies, R. Iribarren in

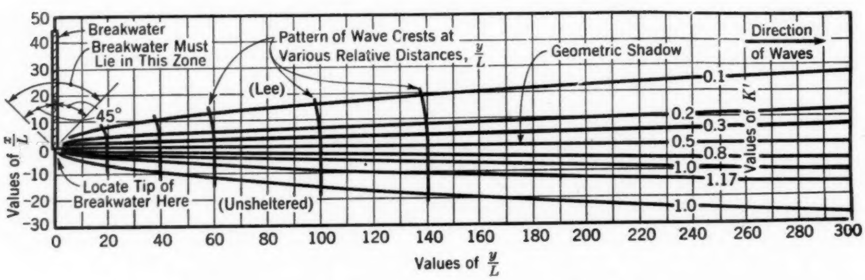

Fig. 11.—Generalized Diffraction Diagram for Tip of Breakwater

[34] "Diffraction of Water Waves by Breakwaters," by J. A. Putnam and R. S. Arthur, *Transactions*, Am. Geophysical Union, Vol. 29, 1948, pp. 481–490.

[35] "Diffraction of Water Waves Passing Through a Breakwater Gap," by F. L. Blue, Jr., and J. W. Johnson, *Transactions*, Am. Geophysical Union, Vol. 30, 1949, pp. 705–718.

[36] "Diffraction of Water Waves by Breakwaters," by J. H. Carr and M. E. Stelzriede, Symposium on Gravity Waves, National Bureau of Standards, Washington, D. C., June, 1951.

[37] "La deformation ondulatoire des jetees verticales," by M. J. Larras, *Travaux*, Vol. 26, June, 1942, pp. 167–170.

Spain,[38] and J. Thysse and J. B. Schijf [39] made experimental studies on diffraction and applied the results to practical design problems. More recently, M. H. Lacombe[40] has made a comparison between the classical hydrodynamic methods of studying wave diffraction and the optical methods of C. Huyghens. In general, the theoretical solutions have been found to apply with conservative results—that is, the predicted wave heights in the lee of a breakwater are found to be slightly larger than the height of waves that may be expected under actual conditions. The use of the diffraction theory in breakwater design is made convenient when summarized in a diagram with curves of equal values of diffraction coefficients on a coordinate system in which the origin of the system is at the tip of a single breakwater or at the center of a gap.[41] The diffraction coefficient in this instance is defined as the ratio of the diffracted wave

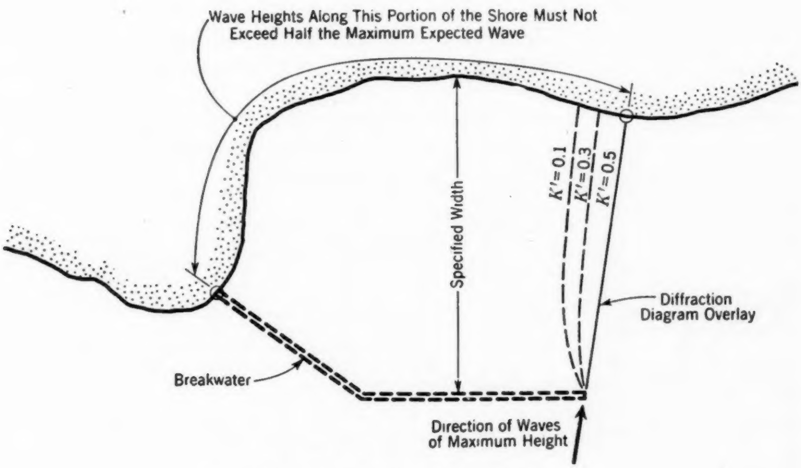

FIG. 12.—USE OF A DIFFRACTION DIAGRAM

height to the incident wave height and is usually designated by the symbol K'. The procedure to be followed in preparing diffraction diagrams appears in the Appendix.

Semi-Infinite Breakwater.—The generalized diffraction diagram shown in Fig. 11 can be applied to a particular breakwater problem once the characteristics of the design wave have been selected—that is, the height, period, and direction of the incident wave from which protection is to be provided. For example, Fig. 12 shows a map of a harbor for which protection is desired for a specified reach of the shore line for waves approaching from the critical direction.

---

[38] "Protection des Ports," by R. C. Iribarren and C. O. Nogales, XVII International Congress, Section II, Communication 4, Lisbon, Portugal, 1949, pp. 31–79.

[39] "Penetration of Waves and Swells into Harbors," by J. Thysse and J. B. Schijf, VII International Navigation Congress, Section II, Communication 4, Lisbon, Portugal, 1949, pp. 151–171.

[40] "Note sur la diffraction de la Houle en incidence normal," by M. H. Lacombe, *Annales Hydrographiques, Separate No. 1363*, Paris, France, 1949, pp. 1–49.

[41] "Generalized Wave Diffraction Diagrams," by J. W. Johnson, Second Conference on Coastal Eng., Houston, Tex., November, 1951.

For the given wave period (or length) a diagram similar to Fig. 11 is plotted on transparent paper to the same length scale as the map of the harbor area. This transparent overlay then is moved over the map, keeping the geometric shadow parallel to the direction of travel until the desired degree of protection for the selected reach of the shore line is obtained. The location of the tip of the breakwater thus is obtained as illustrated by the final location of the overlay shown in Fig. 12.

Diffraction at a Breakwater Gap.—The treatment of diffraction problems, as discussed in the preceding section, is concerned with waves moving past a breakwater tip with an infinite expanse of water existing away from the tip. In many harbors, however, waves move through a relatively narrow gap in a breakwater, hence, diffraction occurs at the two sides of the gap and changes in wave height in the lee of the breakwater; hence, it will be different than if a single tip existed. Theories for this condition also have been developed. An experimental study verified the general form of these theories for breakwater gaps with a ratio of gap-width to wave length as small as 0.5.[35,36]

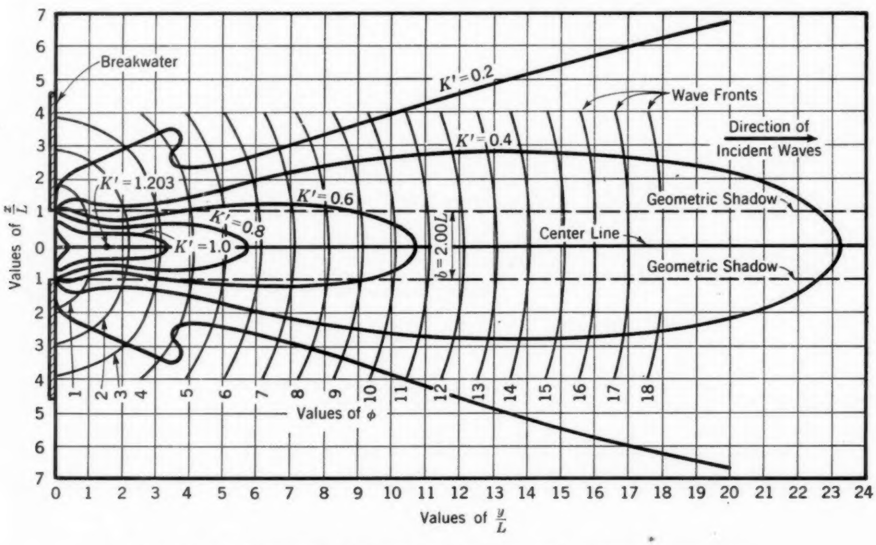

FIG. 13.—GENERALIZED DIFFRACTION DIAGRAM FOR A BREAKWATER GAP

As an illustration of a generalized diagram that gives diffraction coefficients to the lee of a breakwater gap, Fig. 13 shows a diagram for the case in which the gap is two wave lengths in width. The method of making the necessary computations of these diffraction coefficients as well as the computations for the position of the wave fronts are shown in the Appendix. These generalized diagrams,[41] when used as transparent overlays, can be moved over a map of a locality to obtain the most desirable protection, similar to the procedure described for the single breakwater.

When the gap width is in excess of about five wave lengths, the diffraction patterns at each side of the opening are more or less independent of each other.

In such cases, the pattern given by Fig. 11 for a semi-infinite breakwater can be used to estimate the height and direction of waves on the leeward side. For these relatively large gap openings the direction of the incident waves with respect to the breakwater alinement can lie anywhere within the zone indicated in Fig. 11 without the diffraction pattern being appreciably affected.

For relatively narrow gaps the experimental work[42] has been concerned with the case in which the angle between the incident wave and the breakwater is less than 20°. Until more experimental data are available, however, it is believed that useful approximations can be made for cases of oblique incidence by drawing a line through the gap center and normal to the incident wave direction, and then computing diffraction coefficients as though the breakwater were along this line—the end of the imaginary gap being at the projections on this line of the true gap ends (Fig. 14).

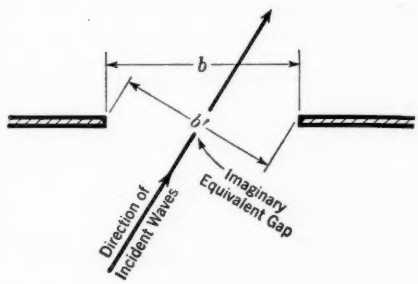

FIG. 14.—WAVE INCIDENCE OBLIQUE TO BREAKWATER GAP

SUMMARY

The application of the principles of refraction and diffraction is of considerable practical importance in the design, construction, operation, and maintenance of many coastal engineering works. These principles permit the estimate of wave conditions at specified points in shallow water or at a shore line from deep-water wave characteristics that are known from either a forecast, a hindcast, or a wave recorder.

APPENDIX

The basic theory of diffraction has been presented elsewhere[34] and need not be discussed in detail in this paper. Basically, the theory assumes: (1) That the waves are of small amplitude compared to the wave length; and (2) that the water is of uniform depth. The first assumption covers the range of wave steepness up to that of storm waves—that is, $H_0/L_0 = 0.03$.

Diffraction by a Vertical Impermeable Semi-Infinite Breakwater.—As mentioned previously, the diffraction coefficient K' is defined as the ratio of diffracted wave height to incident wave height. The value of K' is a function of position with respect to the breakwater, that is,

$$K' = f(u_1) \qquad (16)$$

In this equation

$$u_1 = \sqrt{\frac{4}{L}\left[\sqrt{(x^2 + y^2)} - y\right]} \qquad (17a)$$

[42] "Diffraction of Water Waves Passing Through a Breakwater Gap," by F. L. Blue, Jr., thesis presented to the University of California, at Berkeley, Calif., in 1948, in partial fulfilment of the requirements for the degree of Doctor of Philosophy.

or

$$\frac{x}{L} = \pm \frac{u_1}{\sqrt{2}} \sqrt{\frac{y}{L} + \frac{u^2_1}{8}} \quad \text{(17b)}$$

Referring to Fig. 15, the plus sign in Eq. 17*b* applies to the region of $-(x/L)$ and the minus sign applies to the $+(x/L)$ region. The evaluation of $K' = f(u_1)$ is obtained from a projection of the Cornu spiral. The values of the factor u_1 for various values of K' are given in Table 2.

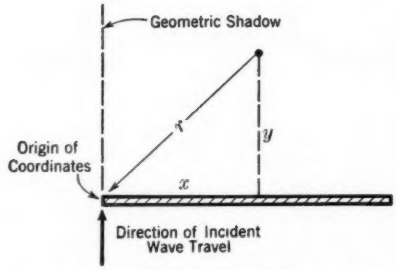

FIG. 15.—WAVE DIFFRACTION ANALYSIS AT BREAKWATER TIP

Eq. 17*b*, used in conjunction with Table 2, permits the construction of a diffraction diagram that shows parabolas of the constant K'. For example, to plot the curve of $K' = 0.2$, the following calculations are made: From Table 2, with $K' = 0.2$, find $u_1 = -1.02$. From Eq. 17*b*, compute $x/L = (-)\,(0.707)\,(-1.02)\,\sqrt{y/L + (0.125)\,(-1.02)^2} = +\,0.722\,\sqrt{y/L + 0.13.}$ The plus sign indicates the region in the lee of the breakwater. The values of x/L now can be computed for various assumed values of relative distance (y/L) using a computation form similar to that outlined in Table 3.

Complete plotting data for various constant values of diffraction coefficients are summarized in Table 4 and plots of these data are shown in Fig. 11. As previously discussed, this figure is a generalized diagram that shows curves of equal values of diffraction coefficients on a coordinate system in which the origin is at the breakwater tip. It is of interest to note on this diagram that along the geometric shadow the wave heights are one half of the height of the incident waves and that waves slightly greater in height than the incident waves are possible beyond the breakwater. This diagram is applicable for a

TABLE 2.—VALUES OF THE TERM u_1

Diffraction coefficient K'	Factor u_1	Crest lag in percentage of wave length L
(*a*) LEE REGION $(+x/L)$		
0.1	−2.25	140
0.15	−1.44	60
0.2	−1.02	33
0.3	−0.528	13
0.4	−0.225	6
(*b*) GEOMETRIC SHADOW REGION		
0.5	0.000	0
(*c*) UNSHELTERED REGION* $(-x/L)$		
0.6	0.184	−3
0.7	0.341	−5
0.8	0.486	−6
0.9	0.631	−5
1.0	0.779	−5
1.17	1.218	0
1.0	1.610	0
0.88	1.878	−3
1.0	2.124	...

uniform depth with either deep-water or shallow-water waves, provided that the proper wave length is used in the particular case. It also applies for conditions in which the angle between the incident wave and the breakwater is other than 90°, as shown by Fig. 11.

In addition to the plot of diffraction coefficients shown in Fig. 11, a plot of wave patterns is desirable in certain investigations. Data for plotting wave patterns are presented in the last column of Table 2, where the lag or lead of the wave front is given. Thus, along the parabola $K' =$ constant, at the corresponding value of (y/L) and (x/L) the wave front will lag (or lead) by the given percentage of the wave length, that portion of the front of the same wave that is at the geometric shadow. It should be recognized that the wave patterns plotted by this method apply only if the water is of uniform depth. Should

TABLE 3.—COMPUTATION FORM FOR DIFFRACTION COEFFICIENTS

$\left(\frac{y}{L}\right)$	$\left(\frac{y}{L}+0.13\right)$	$\sqrt{\left(\frac{y}{L}+0.13\right)}$	$\frac{x}{L}$
5	5.13	2.27	1.64
10	10.13	3.18	2.30
15	15.13	3.89	2.80

TABLE 4.—VALUES OF COORDINATE $\frac{x}{L}$ FOR DIFFRACTION AT THE END OF A SEMI-INFINITE BREAKWATER

Coordinate y/L	Diffraction Coefficient K'						
	Lee or + Values		Geometric Shadow	Unsheltered or − Values			
	0.1	0.2	0.5	0.8	1.0	1.17	1.0
5	3.78	1.64	0.00	0.77	1.24	1.96	3.54
10	5.19	2.30	0.00	1.09	1.75	2.75	4.89
15	6.29	2.80	0.00	1.33	2.14	3.36	5.93
20	7.23	3.23	0.00	1.54	2.47	3.87	6.82
30	8.81	3.95	0.00	1.88	3.02	4.74	8.31
40	10.13	4.56	0.00	2.17	3.49	5.46	9.58
50	11.31	5.10	0.00	2.43	3.90	6.11	10.68
60	12.38	5.59	0.00	2.66	4.27	6.68	11.70
70	13.37	6.04	0.00	2.87	4.61	7.22	12.62
80	14.28	6.46	0.00	3.07	4.93	7.71	13.48
90	15.14	6.85	0.00	3.26	5.23	8.18	14.30
100	15.91	7.22	0.00	3.44	5.51	8.62	15.03
120	17.43	7.90	0.00	3.76	6.04	9.44	16.47
140	18.83	8.53	0.00	4.07	6.52	10.20	17.79
160	20.13	9.13	0.00	4.34	6.97	10.90	19.03
180	21.35	9.68	0.00	4.61	7.40	11.55	20.16
200	22.50	10.20	0.00	4.86	7.80	12.18	21.24
220	23.59	10.70	0.00	5.10	8.18	12.78	22.27
240	24.64	11.18	0.00	5.32	8.54	13.34	23.27
260	25.66	11.63	0.00	5.54	8.89	13.89	24.21
280	26.62	12.07	0.00	5.75	9.23	14.42	25.13
300	27.56	12.50	0.00	5.95	9.55	14.92	26.01

these waves, after passing the breakwater, move into shoaling water in which the bottom contours are not normal to the wave directions, refraction as well as diffraction must be considered; in fact, after a few wave lengths beyond the

barrier, refraction may be more important than diffraction if the depth is changing rapidly. One possible method for treating such problems has been suggested,[42] but further experimental studies in this field appear desirable.

Diffraction at a Breakwater Gap.—A theory for this problem has been discussed elsewhere,[35] and only a summary and an illustrated example need be presented herein. For any position (x, y) as illustrated in Fig. 16, the diffraction coefficient is given by the expression:

$$K' = [F\,(x, y)] \quad \ldots\ldots (18)$$

and

$$\text{Phase Difference} = \arg\,(F \text{ for diffracted wave} + k\,y) \quad \ldots\ldots (19)$$

in which arg denotes argument and $k = 2\,\pi/L$.

In Eq. 18, for $x \leqq b/2$,

$$F\,(x, y) = e^{-i\,k\,y} - f_1 + g_1 - f_2 + g_2 \quad \ldots\ldots (20a)$$

and for $x \geqq b/2$ and $y \geqq 0$,

$$F\,(x, y) = f_1 + g_1 - f_2 + g_2 \quad \ldots\ldots (20b)$$

At $x = b/2$ (geometric shadow) these expressions, of course, are identical. The factors in Eqs. 20 are computed in terms of real and imaginary components, each of which are added arithmetically and combined into a resultant $F\,(x, y)$. The terms f and g in Eq. 20 are defined as follows:

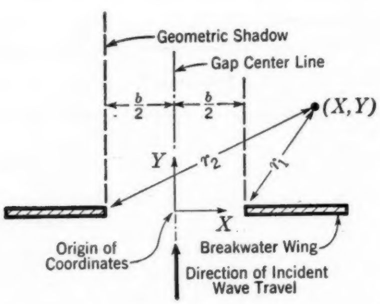

FIG. 16.—WAVE DIFFRACTION ANALYSIS FOR BREAKWATER GAP

$$f = f\,(r, y) = e^{-i\,k\,y} \times f\,(-\,u) \quad \ldots (21)$$

and

$$g = f\,(r, -\,y) = e^{i\,k\,y} \times f\,(-\,u) \quad \ldots (22)$$

in which

$$f\,(-\,u) = S + i\,w$$

S and w are, respectively, the real and imaginary components of $f\,(-\,u)$ and $i = \sqrt{-\,1}$. The term u is defined by the expression,

$$u = \sqrt{\frac{4\,(r - y)}{L}} \quad \ldots\ldots (23)$$

Values of S and w[42] as functions of the quantity u^2 are shown in Fig. 17.

The diffraction coefficient and phase difference at any point (x, y) for a particular breakwater gap of width b are computed by using Eqs. 20 in the following steps. Values of r_1 and r_2 are first obtained from relationships that are

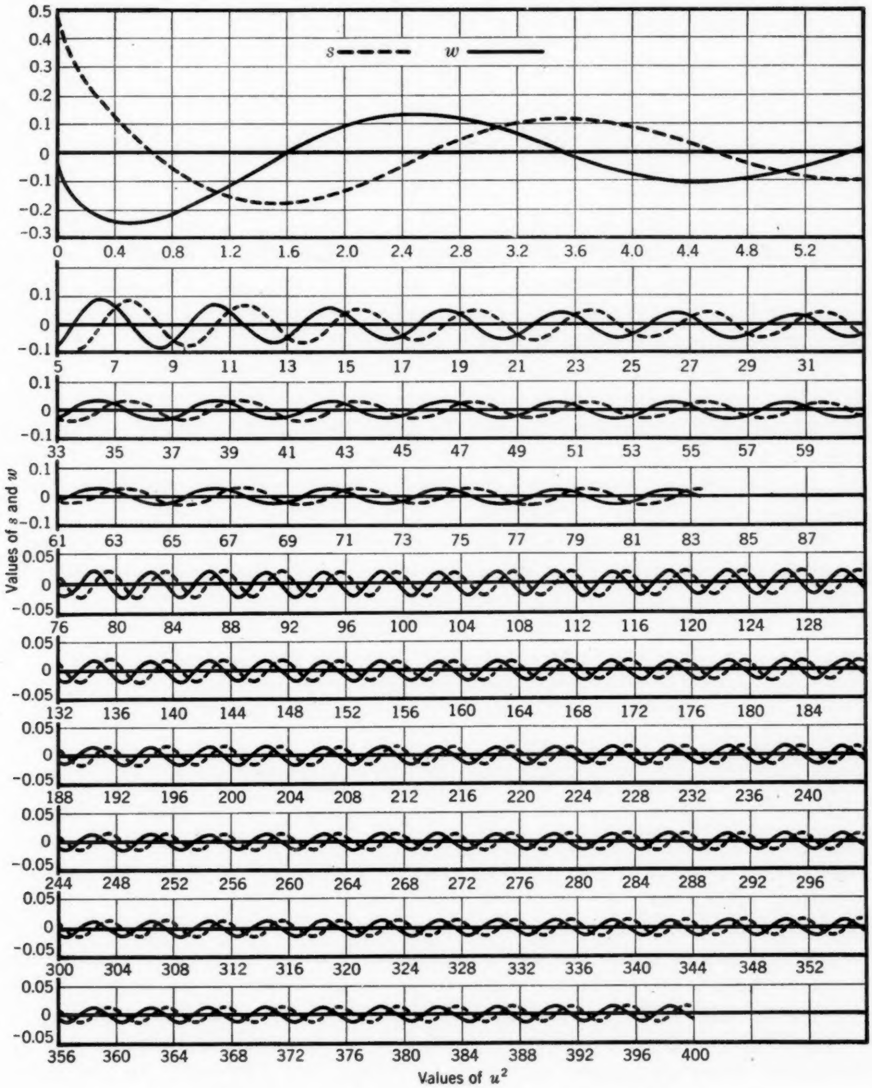

FIG. 17.—CHART FOR DETERMINING VALVES OF FACTORS S AND w

readily derived from the geometry of the system shown in Fig. 16. These are:

$$r_1 = \sqrt{y^2 + \left(x - \frac{b}{2}\right)^2} \text{ for } x \geqq \frac{b}{2} \ldots\ldots\ldots\ldots\ldots (24a)$$

$$r_1 = \sqrt{y^2 + \left(\frac{b}{2} - x\right)^2} \text{ for } x \leqq \frac{b}{2} \ldots\ldots\ldots\ldots\ldots (24b)$$

and

$$r_2 = \sqrt{y^2 + \left(x + \frac{b}{2}\right)^2} \ldots\ldots\ldots\ldots\ldots\ldots\ldots\ldots (25)$$

Values of r_1 and r_2 from these equations are used in Eq. 23 to determine the values of u_1 and u_2, respectively. The values of S_1 and w_1 corresponding to u_1 and S_2 and w_2 corresponding to u_2 are then obtained from Fig. 17. These functions are used in determining f_1 and f_2 by Eq. 21.

A similar procedure is used in determining the value of g_1 and g_2 using Eq. 22. For a given value of x and y, values of u_3 and u_4 are first determined from Eq. 23, in which the value of r_1 and the negative value of y yields u_3, and the value of r_2 and the negative value of y yields u_4. The pair of values (S_3 and w_3) and (S_4 and w_4) corresponding to u_3 and u_4, respectively, are determined from Fig. 17.

In adding the components ($f_1, f_2, g_1,$ and g_2) the difference in phase between f_1 and f_2 (as given by Eq. 21) and g_1 and g_2 (given by Eq. 22) has to be considered. Thus,

$$f_1 = e^{-i\,k\,y} f\,(-\,u_1)$$

and

$$g_1 = e^{i\,k\,y} f\,(-\,u_2) = e^{2\,i\,k\,y}\left[e^{-i\,k\,y} f\,(-\,u_2)\right]$$

That is, there is a phase difference corresponding to the factor $e^{2\,i\,k\,y}$, or $2\,k\,y$. Therefore, in obtaining $\pm f_1 + g_1$ (disregarding the factor $e^{-i\,k\,y}$) from $f\,(-\,u_1)$ and $f\,(-\,u_2)$, the real and imaginary components of $f\,(-\,u_2)$ must be rotated through the angle $2\,k\,y = 4\,\pi\,y/L = 720\,y/L$ degrees and then resolved into components parallel to the real and imaginary components of $f\,(-\,u_1)$ before addition. Similarly, $f\,(-\,u_4)$ must be rotated through the same angle α. To perform this operation numerically, the factors $\cos\alpha$ and $-\sin\alpha$ are applied to the real and imaginary parts, respectively, of $f\,(-\,u_2)$ and $f\,(-\,u_4)$, which then are added to obtain the components to be added to the real parts of $\pm f\,(-\,u_1)$ and $-f\,(-\,u_3)$; while the factors $\sin\alpha$ and $\cos\alpha$ are applied to the real and imaginary parts of $f\,(-\,u_2)$ and $f\,(-\,u_4)$ to obtain the components to be added to the imaginary parts of $\pm f\,(-\,u_1)$ and $f\,(-\,u_3)$. In the same manner, the term $e^{-i\,k\,y}$, takes the value $1 + i$ in the addition.

Designating the sum of the real components S and that of the imaginary components w, the value of the diffraction coefficient $K' = [F\,(x, y)]$ is obtained from

$$K' = \sqrt{w^2 + S^2} \ldots\ldots\ldots\ldots\ldots\ldots\ldots\ldots (26)$$

and the phase difference caused by diffraction is

$$\text{phase difference} = \tan^{-1}\left(\frac{w}{S}\right) \quad (27)$$

In the practical case the diffraction coefficients and phase differences are calculated for a breakwater gap of width b with waves of wave length L approaching parallel to the breakwater. Instead of making computations for specific values of b and L, the results can be generalized by considering values of b, x, and y as multiples of the wave length L. Thus, computations of diffraction coefficients and phase differences are made for a given ratio of gap-width to wave length at various relative positions x/L and y/L in the lee of the breakwater. For convenience in computations, Eq. 24 and Eq. 25 with $x \geqq \frac{b}{2}$ are written:

$$\frac{r_1}{L} = \sqrt{\left(\frac{y}{L}\right)^2 + \left(\frac{x}{L} - \frac{b}{2L}\right)^2} \quad (28a)$$

$$\frac{r_2}{L} = \sqrt{\left(\frac{y}{L}\right)^2 + \left(\frac{x}{L} + \frac{b}{2L}\right)^2} \quad (28b)$$

Values u_1^2, u_2^2, u_3^2, and u_4^2, therefore, are computed for various values of $\frac{x}{L}$ and $\frac{y}{L}$ from Eq. 23 transformed as follows:

$$u_1^2 = 4\left(\frac{r_1}{L} - \frac{y}{L}\right) \quad (29a)$$

$$u_2^2 = 4\left(\frac{r_2}{L} - \frac{y}{L}\right) \quad (29b)$$

$$u_3^2 = 4\left(\frac{r_1}{L} + \frac{y}{L}\right) \quad (29c)$$

$$u_4^2 = 4\left(\frac{r_2}{L} + \frac{y}{L}\right) \quad (29d)$$

TABLE 5.—COMPUTATION OF ANGLE α

Assumed value of n (1)	y/L (2)	$y/L - n/2$ (3)	$\alpha = 720(y/L - n/2)$ degrees (4)	Sin α (5)	Cos α (6)
1	0.6	0.1	72	+0.951	+0.309
3	1.8	0.3	216	−0.588	−0.809
5	3.0	0.5	360	0	+1.000
7	4.2	0.7	144[a]	+0.588	−0.809
10	6.0	1.0	—	0	+1.000
20	12.0	2.0	—	0	+1.000
30	18.0	3.0	—	0	+1.000
50	30.0	5.0	—	0	+1.000

[a] 504° = 144°.

From Fig. 17, values of S and w are obtained, and the diffraction coefficients and phase differences are then computed.

Numerical Example.—A generalized diagram is to be drawn for diffraction at a breakwater gap whose width is two wave lengths. Thus, $b/L = 2$.

As an illustration, Tables 5 and 6 give a typical setup for computation of diffraction coefficients and phase differences at various positions y/L ranges 0, 1, 2, and 3 from the gap. The positions y/L have been arbitrarily assumed to be multiples "m" of an initial value of $y/L = 0.6$. The sequence of the steps in the calculation process in Tables 5 and 6 is self explanatory. A plot of the diffraction coefficients can be made directly from the data shown in Table 6, from which contours of equal diffraction coefficients can then be constructed, as shown in Fig. 13.

TABLE 6.—Calculation of Diffraction Coefficient for Breakwater Gap

Assumed Value of n	y/L	$\frac{r_1}{L}$ [a]	u_1^2 [b]	f_1 [c]		u_3^2 [d]	g_1 [c]		$\frac{r_2}{L}$ [e]	u_2^2 [f]	f_2 [c]		u_4^2 [g]	g_2 [c]		M [h] [i]
				S_1	w_1		S_3	w_3			S_2	w_2		S_4	w_4	
(1)	(2)	(3)	(4)	(5)	(6)	(7)	(8)	(9)	(10)	(11)	(12)	(13)	(14)	(15)	(16)	(17)
(a) $x/L = 2$ $(K' = f_1 + g_1 - f_2 + g_2)$																
1	0.6	1.166	2.26	−0.069	+0.131	7.06	+0.062	+0.062	3.06	9.84	−0.065	+0.035	14.64	+0.015	+0.057	+0.077
3	1.8	2.06	1.04	−0.116	−0.158	15.44	+0.054	+0.008	3.50	6.80	+0.038	+0.080	21.2	−0.042	−0.025	+0.012
5	3.0	3.16	0.64	+0.013	−0.235	24.6	−0.006	−0.043	4.24	4.96	−0.061	−0.076	29.0	−0.028	−0.029	−0.034
7	4.2	4.32	0.48	+0.096	−0.245	34.1	−0.022	+0.032	5.16	3.84	+0.103	−0.049	37.4	−0.033	−0.006	−0.055
10	6.0	6.08	0.32	+0.175	−0.230	48.3	+0.010	−0.030	6.71	2.84	+0.055	+0.120	50.8	+0.015	+0.030	+0.025
20	12	12.04	0.16	+0.282	−0.184	96.2	+0.010	−0.021	12.37	1.48	−0.169	−0.034	97.5	−0.021	−0.001	−0.011
30	18	18.028	0.112	+0.327	−0.156	144.1	+0.011	−0.014	18.25	1.00	−0.106	−0.167	145.0	−0.013	−0.012	−0.002
50	30	30.017	0.068	+0.365	−0.126	240.1	+0.008	−0.012	30.15	0.60	+0.031	−0.239	240.6	−0.002	−0.014	+0.006
(b) $x/L = 1 = \frac{b}{2}$ Geometric Shadow $(K' = f_1 + g_1 - f_2 + g_2)$																
1	0.6	0.600	0.000	+0.500	0.000	4.80	−0.042	−0.091	2.09	5.96	−0.074	+0.059	10.76	+0.026	+0.053	−0.016
3	1.8	1.800	0.000	+0.500	0.000	14.40	−0.011	+0.057	2.69	3.56	+0.119	0.000	17.96	−0.037	+0.034	−0.048
5	3.0	3.00	0.000	+0.500	0.000	24.0	+0.034	−0.032	3.61	2.44	−0.028	+0.140	26.44	−0.005	+0.040	+0.029
7	4.2	4.20	0.000	+0.500	0.000	33.6	−0.038	+0.006	4.65	1.80	−0.149	+0.054	35.4	+0.032	+0.007	−0.006
10	6.0	6.00	0.000	+0.500	0.000	48.0	+0.023	−0.024	6.33	1.32	−0.161	−0.081	49.3	−0.029	−0.008	−0.006
20	12	12.00	0.000	+0.500	0.000	96.0	+0.017	−0.017	12.17	0.68	−0.012	−0.230	96.7	−0.006	−0.022	+0.011
30	18	18.00	0.000	+0.500	0.000	144.0	+0.013	−0.012	18.11	0.44	+0.106	−0.244	144.4	+0.003	−0.018	+0.016
50	30	30.00	0.000	+0.500	0.000	240.0	+0.011	−0.011	30.07	0.28	+0.197	−0.233	240.3	+0.005	−0.015	+0.016
(c) $x/L = 0$ $(K' = e^{-iky} - f_1 + g_1 - f_2 + g_2)$																
1	0.6	1.166	2.26	−0.069	+0.131	7.06	+0.062	+0.062	1.116	2.26	−0.069	+0.131	7.06	+0.062	+0.062	+0.124
3	1.8	2.06	1.04	−0.116	−0.158	15.44	+0.054	+0.008	2.06	1.04	−0.116	−0.158	15.44	+0.054	+0.008	+0.108
5	3.0	3.16	0.64	+0.013	−0.235	24.6	−0.006	−0.043	3.16	0.64	+0.013	−0.235	24.6	−0.006	−0.043	−0.012
7	4.2	4.32	0.48	+0.086	−0.245	34.1	−0.022	+0.032	4.32	0.48	+0.086	−0.245	34.1	−0.022	+0.032	−0.044
10	6.0	6.08	0.32	+0.175	−0.230	48.3	+0.010	+0.030	6.08	0.32	+0.175	−0.230	48.3	+0.010	−0.030	+0.020
20	12	12.04	0.16	+0.282	−0.184	96.2	+0.010	−0.021	12.04	0.16	+0.282	−0.184	96.2	+0.010	−0.021	+0.020
30	18	18.028	0.112	+0.327	−0.156	144.1	+0.011	−0.014	18.028	0.112	+0.327	−0.156	144.1	+0.011	−0.014	+0.022
50	30	30.017	0.068	+0.365	−0.126	240.1	+0.008	−0.012	30.017	0.068	+0.365	−0.126	240.1	+0.008	−0.012	+0.016
(d) $x/L = 3$ $(K' = f_1 + g_1 - f_2 + g_2)$																
1	0.6	2.09	5.96	−0.074	+0.059	10.76	+0.025	+0.063	4.045	13.78	−0.057	+0.025	18.58	+0.007	+0.024	+0.032
3	1.8	2.69	3.56	+0.119	0.000	17.96	−0.038	+0.034	4.39	10.36	−0.018	+0.066	24.76	−0.015	−0.041	−0.053
5	3.0	3.61	2.44	−0.028	+0.140	26.44	−0.005	+0.040	5.00	8.00	+0.060	−0.053	32.00	+0.027	−0.026	+0.022
7	4.2	4.65	1.80	−0.149	+0.054	35.4	+0.032	+0.007	5.80	6.40	−0.019	+0.086	40.0	+0.026	+0.023	+0.058
10	6.0	6.33	1.32	−0.161	−0.081	49.3	−0.029	−0.008	7.21	4.84	−0.043	−0.089	52.89	−0.014	−0.028	−0.043
20	12	12.166	0.66	+0.004	−0.233	96.7	−0.005	−0.022	12.65	2.60	+0.006	+0.138	98.6	+0.003	+0.023	−0.002
30	18	18.111	0.44	+0.106	−0.244	144.4	+0.003	−0.018	18.44	1.76	−0.153	+0.044	145.8	−0.016	+0.009	−0.013
50	30	30.067	0.27	+0.202	−0.220	240.3	+0.005	−0.015	30.266	1.064	−0.123	−0.150	241.1	−0.011	−0.007	−0.006

[a] Eq. 28a. [b] Eq. 29a. [c] Fig. 17. [d] Eq. 29c. [e] Eq. 28b. [f] Eq. 29b [g] Eq. 29d. [h] $M = S_3 + S_4$. [i] Continued in Col. 18 to 32.

TABLE 6.—(*Continued*)

Assumed Value of n (1)	N[j] [k] (18)	$M \cos \alpha$[l] (19)	$-N \sin \alpha$[l] (20)	$S_1 - S_2$ (21)	ΣS (22)	$M \sin \alpha$[l] (23)	$N \cos \alpha$[l] (24)	$w_1 - w_2$ (25)	Σw (26)	w^2 (27)	S^2 (28)	K'[m] (29)	$\frac{w}{S}$ (30)	Phase[n] difference, degrees (31)	$\frac{y}{L}$ (32)
(a) $x/L = 2$ $(K' = f_1 + g_1 - f_2 + g_2)$															
1	+0.119	+0.024	−0.113	−0.004	−0.093	+0.073	+0.037	+0.096	+0.206	0.0424	0.0086	0.226	− 2.215	+114.3	0.6
3	−0.017	−0.009	−0.010	−0.154	−0.173	−0.007	+0.014	−0.238	−0.231	0.0534	0.0299	0.289	+ 1.335	−126.8	1.8
5	−0.072	−0.034	0.000	+0.074	+0.040	0.000	−0.072	−0.159	−0.231	0.0534	0.0016	0.235	− 5.675	− 80.2	3.0
7	+0.026	+0.045	−0.015	−0.017	+0.013	−0.032	−0.021	−0.196	−0.249	0.0620	0.0002	0.249	−19.15	− 87.0	4.2
10	0.000	+0.025	0.000	+0.120	+0.145	0.000	0.000	−0.350	−0.350	0.1225	0.0210	0.379	− 2.414	− 67.5	6.0
20	−0.022	−0.011	0.000	+0.451	+0.440	0.000	−0.022	−0.150	−0.172	0.0296	0.1936	0.472	− 0.3909	− 21.4	12
30	−0.026	−0.002	0.000	+0.433	+0.431	0.000	−0.026	+0.011	−0.015	0.0002	0.1858	0.431	− 0.0348	− 2.0	18
50	−0.026	+0.006	0.000	+0.334	+0.340	0.000	−0.026	+0.113	+0.087	0.0076	0.1156	0.351	+ 0.2559	+ 14.4	30
(b) $x/L = 1 = \frac{b}{2}$ Geometric Shadow $(K' = f_1 + g_1 - f_2 + g_2)$															
1	−0.038	−0.005	+0.036	+0.574	+0.605	−0.015	−0.012	−0.059	−0.086	0.0074	0.3660	0.611	− 0.1421	− 8.1	0.6
3	+0.091	+0.039	+0.053	+0.381	+0.473	+0.028	−0.074	0.000	−0.046	0.0021	0.2237	0.475	− 0.0973	− 5.6	1.8
5	+0.008	+0.029	0.000	+0.528	+0.577	0.000	+0.008	−0.140	−0.132	0.0174	0.3102	0.572	− 0.2370	− 13.3	3.0
7	+0.013	+0.005	0.000	+0.649	+0.646	−0.004	−0.011	−0.054	−0.069	0.0048	0.4173	0.650	− 0.1068	− 6.1	4.2
10	−0.032	−0.006	0.000	+0.661	+0.655	0.000	−0.032	+0.081	+0.049	0.0024	0.4290	0.657	+ 0.0748	+ 4.3	6.0
20	−0.039	+0.011	0.000	+0.512	+0.523	0.000	−0.039	+0.230	+0.191	0.0365	0.2735	0.557	+ 0.3652	+ 20.1	12
30	−0.030	+0.016	0.000	+0.394	+0.410	0.000	−0.030	+0.244	+0.214	0.0458	0.1681	0.463	+ 0.5220	+ 27.6	18
50	−0.026	+0.016	0.000	+0.303	+0.319	0.000	−0.026	+0.223	+0.197	0.0388	0.1018	0.375	+ 0.6176	+ 31.7	30
(c) $x/L = 0$ $(K' = e^{-iky} - f_1 + g_1 - f_2 + g_2)$															
1	+0.124	+0.038	−0.118	+1.138[o]	+1.058	+0.118	+0.038	−0.262[p]	−0.106	0.0112	1.1194	1.063	− 0.1002	− 5.7	0.6
2	+0.016	−0.087	+0.009	+1.232	+1.154	−0.063	−0.013	+0.316	+0.240	0.0576	1.3317	1.179	+ 0.2080	+ 11.8	1.8
5	−0.086	−0.012	0.000	+0.974	+0.962	0.000	−0.086	+0.470	+0.384	0.1475	0.9254	1.036	+ 0.3992	+ 21.8	3.0
7	+0.064	+0.036	−0.038	+0.828	+0.826	−0.026	−0.042	+0.490	+0.412	0.1697	0.6823	0.923	+ 0.4998	+ 26.5	4.2
10	−0.060	+0.020	0.000	+0.650	+0.670	0.000	−0.060	+0.460	+0.400	0.1600	0.4489	0.780	+ 0.5970	+ 30.8	6.0
20	−0.052	+0.020	0.000	+0.436	+0.456	0.000	−0.042	+0.363	+0.326	0.1063	0.2074	0.561	+ 0.7149	+ 35.6	12
30	−0.028	+0.022	0.000	+0.346	+0.368	0.000	−0.028	+0.312	+0.284	0.0807	0.1354	0.465	+ 0.7717	+ 37.7	18
50	−0.024	+0.016	0.000	+0.270	+0.286	0.000	−0.024	+0.252	+0.228	0.0520	0.0818	0.366	+ 0.7972	+ 38.6	30
(d) $x/L = 3$ $(K' = f_1 + g_1 - f_2 + g_2)$															
1	+0.087	+0.010	−0.083	−0.017	−0.090	+0.030	+0.027	+0.034	+0.091	0.0083	0.0081	0.128	− 1.0111	+134.7	0.6
3	−0.007	+0.043	−.0004	+0.137	+0.176	+0.031	+0.006	−0.066	+0.029	0.0008	0.0310	0.178	− 0.1648	− 9.4	1.8
5	+0.014	+0.022	0.000	−0.088	−0.066	0.000	+0.014	+0.193	+0.207	0.0428	0.0044	0.217	− 3.1364	+107.7	3.0
7	−0.016	−0.047	+0.009	−0.130	−0.168	+0.034	+0.013	−0.032	+0.015	0.0002	0.0282	0.169	− 0.0892	+174.9	4.2
10	−0.036	−0.043	0.000	−0.118	−0.161	0.000	−0.036	+0.008	+0.028	0.0008	0.0259	0.163	+ 0.1739	−170.1	6.0
20	+0.001	−0.002	0.000	−0.002	−0.004	0.000	+0.001	−0.371	+0.370	0.1369	0.0000	0.370	+92.50	− 90.6	12
30	−0.009	−0.013	0.000	+0.259	+0.246	0.000	−0.009	−0.288	−0.297	0.0882	0.0605	0.386	− 1.2073	− 50.4	18
50	−0.022	−0.006	0.000	+0.325	+0.319	0.000	−0.022	−0.070	−0.092	0.0085	0.1018	0.332	− 0.2884	− 16.1	30

[j] $N = w_3 + w_4$. [k] Continued from Col. 1 to 17. [l] Sin α and Cos α from Table 5. [m] $K' = \sqrt{w^2 + s^2}$. [n] Eq. 27. [o] Values in this section of Col. 21 are computed using $1 - S_1 - S_2$. [p] Values in this section of Col. 25 are computed using $-w_1 - w_2$.

A plot of the wave patterns in the lee of the breakwater gap involves additional computations. The "phase difference," as computed in Table 6, is that of Eq. 19, with complete cycles omitted. To express this phase difference in terms of complete cycles, it must be divided by 360°. To obtain the complete phase, the phase of the incident wave must be added to the phase difference.

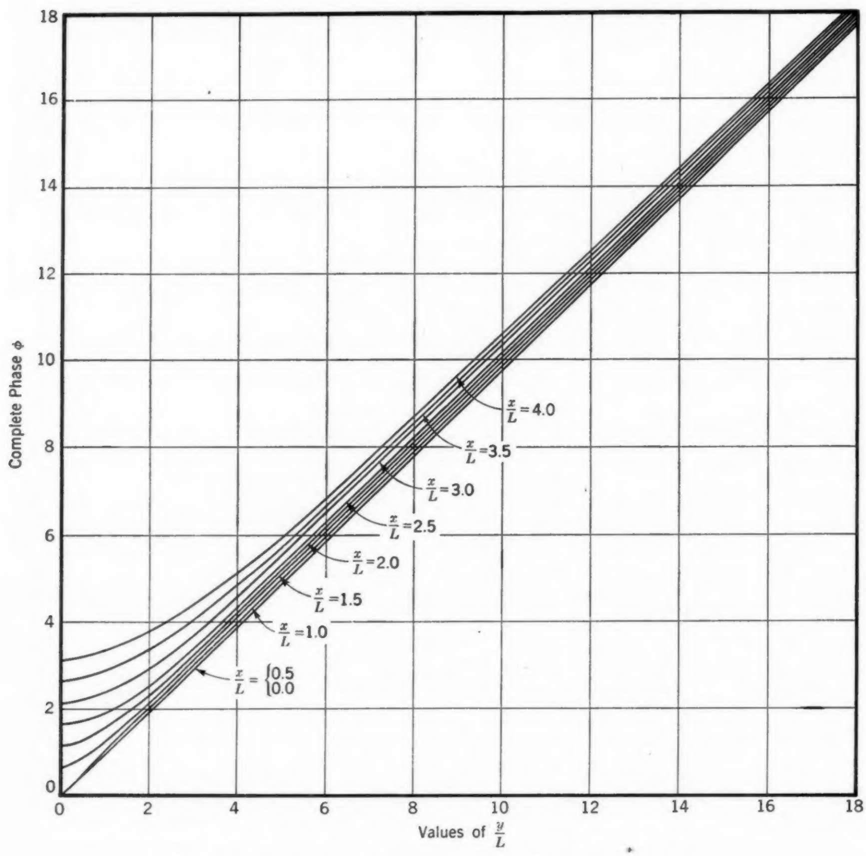

FIG. 18.—BREAKWATER DIFFRACTION FOR GAP WIDTH $b/L = 2$

The phase of the incident wave also is expressed in cycles, that is $\frac{-y}{L+m}$, in which m is an integer. The whole cycles are omitted, both phases being expressed as negative angles, thus indicating a decrease in phase as y increases. In the computations for complete phase for various positions (x/L, y/L) it is usually convenient to make a plot of the phase, ϕ, against values of y/L, as shown in Fig. 18. Since the curve for $x/L = 0$ rises at slightly less than 45°, a 45° line is first drawn lightly on the plot, thus making clear the value of the integer m (or the whole number of cycles) to be added to the phase difference. The computation procedure in arriving at the complete phase is illustrated in

Table 7. Thus, for various of y/L and x/L the corresponding values of phase difference (PD), as computed and shown in col. 31 of Table 6 were first tabulated (minus values of phase difference were subtracted from 360° before tabulation in Table 7. These values of PD were next divided by 360°. Referring to Fig. 18, the integer m was obtained for each value of y/L (for example, for $y/L = 3$, the value of m is equal to the first integer below the $x/L = 0$ line, which is 2). Values of m for the various values of y/L are shown in Table 7.

TABLE 7.—TYPICAL COMPUTATION FOR COMPLETE PHASE

m	y/L	Phase difference, degrees	Col. 3 ÷ 360	Complete phase[a]	Phase difference, degrees	Col. 3 ÷ 360	Complete phase[a]	Phase difference, degrees	Col. 3 ÷ 360	Complete phase[a]
(1)	(2)	(3)	(4)	(5)	(3)	(4)	(5)	(3)	(4)	(5)
		(a) $x/L = 0$			(b) $x/L = 1$			(c) $x/L = 2$		
1	0	360	1.000	0	360	1.000	0	319.7	0.888	0.112
−1	0.6	354.3	0.984	0.616	352.2	0.978	0.622	114.3	0.318	0.282
1	1.8	11.8	0.033	0.767	354.4	0.984	0.816	232.9	0.647	0.153
2	3.0	21.8	0.061	0.939	346.7	0.963	0.037	279.8	0.777	0.223
4	4.2	26.5	0.074	0.126	353.9	0.983	0.217	273.0	0.758	0.442
5	6.0	30.8	0.086	0.914	4.3	0.012	0.988	292.5	0.813	0.187
8	9.0	33.9	0.094	0.906	15.3	0.042	0.958	320.5	0.890	0.110
11	12	35.6	0.099	0,901	20.1	0.056	0.944	338.6	0.941	0.059
14	15	36.9	0.102	0.898	23.4	0.065	0.935	352.0	0.978	0.022
17	18	37.7	0.105	0.895	27.6	0.077	0.923	358.0	0.994	0.006

[a] $-\frac{PD}{360} + \frac{y}{L} - m.$

TABLE 8.—BREAKWATER DIFFRACTION TABULATION

Values of ϕ	Values of y/L: 0	0.5	1.0	1.5	2.0	2.5	3.0	3.5	4.0
0	0	0	0	—	—	—	—	—	—
1	1.00	1.00	0.95	0.75	—	—	—	—	—
2	2.05	2.05	1.95	1.90	1.65	1.10	—	—	—
3	3.10	3.10	3.00	2.90	2.75	2.50	2.05	1.30	—
4	4.05	4.05	4.00	3.90	3.75	3.65	3.35	3.00	2.45
5	5.05	5.05	5.00	4.85	4.75	4.70	4.50	4.25	3.85
6	6.10	6.10	6.00	5.90	5.80	5.70	5.50	5.35	5.05
7	7.10	7.10	7.00	6.95	6.85	6.70	6.55	6.40	6.20
8	8.10	8.10	8.05	7.95	7.85	7.75	7.60	7.45	7.20
9	9.10	9.10	9.05	8.95	8.90	8.80	8.65	8.50	8.25
10	10.10	10.10	10.05	10.00	9.90	9.80	9.70	9.55	9.30
11	11.10	11.10	11.05	11.00	10.95	10.85	10.75	10.60	10.40
12	12.10	12.10	12.05	12.00	11.95	11.85	11.75	11.60	11.45
13	13.10	13.10	13.05	13.00	12.95	12.90	12.80	12.65	12.50
14	14.10	14.10	14.05	14.00	13.95	13.90	13.80	14.70	13.55
15	15.10	15.10	15.05	15.00	15.00	14.90	14.80	14.70	14.60
16	16.10	16.10	16.05	16.05	16.00	15.95	15.85	15.75	15.60
17	17.10	17.10	17.05	17.05	17.00	16.95	16.85	16.75	16.65
18	—	—	—	—	18.00	17.95	17.85	17.75	17.65

The remaining steps consist of the summation of the terms $(-\overline{\text{PD}}/360)$, (y/L) and $-m$, for each value of x/L, using

$$\frac{-\text{PD}}{360} + \frac{y}{L} - m = \text{complete phase} \qquad (30)$$

The remaining curves of phase (for x/L = constant) now may be drawn by starting at $x/L = 0$ with phases taken from Table 7, due allowance being made for the value of m, or the complete cycles. Each curve of (x/L = constant) lies above and approximately parallel to the preceding curve as higher values of y/L are used.

Points for the wave pattern are computed by noting from the curves shown in Fig. 18 the values of y/L at which the phases for x/L = constant reached integral values. These points are tabulated in Table 8. Wave patterns now may be drawn as curves joining the points having the same integral phases. The patterns for the gap width of 2 L are shown in Fig. 13, together with the contours of equal diffraction coefficients.

CURRENT PAPERS AND DISCUSSIONS

Proceedings-Separate Number	Date Available	Title and Author	Discussion closes
87	Oct., 1951	"Sewage Reclamation by Spreading Basin Infiltration," by Ralph Stone and William F. Garber	Mar. 1
88	Oct., 1951	"Experimental Study of Water Flow in Annular Pipes," by W. M. Owen	Mar. 1
89	Oct., 1951	"Deflections in Gridworks and Slabs," by Walter W. Ewell, Shigeo Okubo, and Joel I. Abrams	Mar. 1
90	Nov., 1951	"Consumptive Use of Water by Forest and Range Vegetation," by L. R. Rich	Apr. 1
91	Nov., 1951	"Consumptive Use of Water," by Harry F. Blaney	Apr. 1
92	Nov., 1951	"Experimental Investigation of Fire Monitors and Nozzles," by Hunter Rouse, J. W. Howe, and D. E. Metzler	Apr. 1
93	Nov., 1951	"Aircraft Design as Related to Airport Standards," by Milton W. Arnold	Apr. 1
94	Nov., 1951	"Friendship International Airport," by Benjamin Everett Beavin	Apr. 1
95	Nov., 1951	"Directional Requirements for Airport Runways," by Ralph H. Burke and Harry Otis Wright, Jr.	Apr. 1
96	Nov., 1951	"Surface Curves for Steady Nonuniform Flow," by Robert B. Jansen	Apr. 1
97	Dec., 1951	"Consumptive Use in the Rio Grande Basin," by Robert L. Lowry	May 1
98	Dec., 1951	"Consumptive Use of Water on Irrigated Land," by Wayne D. Criddle	May 1
99	Dec., 1951	"Consumptive Use in Municipal and Industrial Areas," by George B. Gleason	May 1
100	Dec., 1951	"Forced Vibrations of Continuous Beams," by Edward Saibel and Elio D'Appolonia	May 1
101	Dec., 1951	"Application of Highway Capacity Research," by J. P. Buckley	May 1
102	Dec., 1951	"Utilization of Ground Water in California," by T. Russel Simpson	May 1
103	Dec., 1951	"Pile Foundations for Large Towers on Permafrost," by L. A. Nees	May 1
104	Dec., 1951	"Redesign of Major Airport Terminals," by Herbert H. Howell	May 1
105	Dec., 1951	"Principles of Highway Capacity Research," by O. K. Normann	May 1
106	Jan., 1952	"Analysis of Ground-Water Lowering Adjacent to Open Water," by Stuart B. Avery, Jr.	June 1
107	Jan., 1952	"Characteristics of the Solitary Wave," by James W. Daily and Samuel C. Stephan, Jr.	June 1
108	Jan., 1952	"Control of Embankment Material by Laboratory Testing," by F. C. Walker and W. G. Holtz	June 1
109	Jan., 1952	"Final Foundation Treatment at Hoover Dam," by A. Warren Simonds	June 1
110	Jan., 1952	"Review of Flood Frequency Methods," Final Report of the Subcommittee of the ASCE Joint Division Committee on Floods	June 1
111	Jan., 1952	"Research in Water Spreading," by Dean C. Muckel	June 1
112	Feb., 1952	"Diversions from Alluvial Streams," by C. P. Linder	July 1
113	Feb., 1952	"Wave Forces on Breakwaters," by Robert Y. Hudson	July 1
114	Feb., 1952	"Utilization of Underground Storage Reservoirs," by Harvey O. Banks	July 1
115	Mar., 1952	"Lake Michigan Erosion Studies," by Colonel John R. Hardin and William H. Booth, Jr.	Aug. 1
116	Mar., 1952	"Graphical Solution of Hydraulic Problems," by Kenneth E. Sorensen	Aug. 1
117	Mar., 1952	"The Development of Stresses in Shasta Dam," by J. M. Raphael	Aug. 1
118	Mar., 1952	"Flocculation Phenomena in Turbid Water Clarification," by W. F. Langelier, Harvey F. Ludwig, and Russell G. Ludwig	Aug. 1
119	Apr., 1952	"Thin-Walled Members in Combined Torsion and Flexure," by Warner Lansing	Sept. 1
120	Apr., 1952	"Surface Water Wave Theories," by Martin A. Mason	Sept. 1
121	Apr., 1952	"Rate of Change of Grade per Station," by Clarence J. Brownell	Sept. 1
122	Apr., 1952	"Engineering Aspects of Diffraction and Refraction," by J. W. Johnson	Sept. 1

AMERICAN SOCIETY OF CIVIL ENGINEERS

OFFICERS FOR 1952

PRESIDENT

CARLTON S. PROCTOR

VICE-PRESIDENTS

Term expires October, 1952:

WILLIAM R. GLIDDEN
DANIEL V. TERRELL

Term expires October, 1953:

GEORGE W. BURPEE
A M RAWN

DIRECTORS

Term expires October, 1952:

MILTON T. WILSON
MORRIS GOODKIND

Term expires January, 1953:

OTTO HOLDEN
FRANK L. WEAVER
GORDON H. BUTLER
G. BROOKS EARNEST
GEORGE W. LAMB
EDWARD C. DOHM

Term expires October, 1953:

KIRBY SMITH
FRANCIS S. FRIEL
WALLACE L. CHADWICK
NORMAN R. MOORE
BURTON G. DWYRE
LOUIS R. HOWSON

Term expires October, 1954:

WALTER D. BINGER
FRANK A. MARSTON
GEORGE W. McALPIN
JAMES A. HIGGS
I. C. STEELE

PAST-PRESIDENTS

Members of the Board

ERNEST E. HOWARD
GAIL A. HATHAWAY

TREASURER

CHARLES E. TROUT

EXECUTIVE SECRETARY

WILLIAM N. CAREY

ASSISTANT TREASURER

GEORGE W. BURPEE

ASSISTANT SECRETARY

E. L. CHANDLER

PROCEEDINGS OF THE SOCIETY

SYDNEY WILMOT
Manager of Technical Publications

HAROLD T. LARSEN
Editor of Technical Publications

COMMITTEE ON PUBLICATIONS

LOUIS R. HOWSON

FRANCIS S. FRIEL
I. C. STEELE
OTTO HOLDEN
FRANK A. MARSTON
NORMAN R. MOORE